Louisiana Transportation Research Center

Final Report 593

Live Load Rating of Cast-in-Place Concrete Box Culverts

by

Ayman M. Okeil, Ph.D., P.E.
Tuna Ulger, Ph.D.
Ahmed Elshoura

LSU

4101 Gourrier Avenue | Baton Rouge, Louisiana 70808
(225) 767-9131 | (225) 767-9108 fax | www.ltrc.lsu.edu

TECHNICAL REPORT STANDARD PAGE

1. Report No.	2. Government Accession No.	3. Recipient's Catalog No.
FHWA/LA.17/593		

4. Title and Subtitle	5. Report Date
Live Load Rating of Cast-in-Place Concrete Box Culverts	July 2018
	6. Performing Organization Code

7. Author(s)	8. Performing Organization Report No.
Ayman M. Okeil, Ph.D., P.E. Tuna Ulger, Ph.D. Ahmed Elshoura	

9. Performing Organization Name and Address	10. Work Unit No.
Department of Civil and Environmental Engineering Louisiana State University Baton Rouge, LA 70803	11. Contract or Grant No. LTRC Project Number: 16-3ST State Project Number: DOTLT1000108

12. Sponsoring Agency Name and Address	13. Type of Report and Period Covered
Louisiana Department of Transportation and Development P.O. Box 94245 Baton Rouge, LA 70804-9245	**Final Report** **2016 –2017**
	14. Sponsoring Agency Code

15. Supplementary Notes

16. Abstract

Cast-in-place (CIP) reinforced concrete (RC) box culverts constitute a large portion of Louisiana's bridge inventory. Culverts constructed using old detailing standards, especially the ones with lower fill heights, typically produce lower load rating factors when AASHTO procedures are followed. Nevertheless, the performance of these culverts is typically acceptable, and they rarely show signs of distress. The purpose of this project is to assess the load rating of representative CIP-RC box culverts from the Louisiana DOTD inventory. Eight culverts with different fill heights and pavement types were selected for the study. In the first phase of this research, field live load testing of the culverts was conducted after instrumenting each culvert with a structural health monitoring (SHM) system consisting of a total 48 sensors including displacement, strain, and tiltmeter sensors. In the second phase of the research, refined three-dimensional (3D) finite element (FE) models were built for each tested culvert and were calibrated using measured field data. AASHTO's Manual for Bridge Evaluation (MBE) rating methodology was followed in this research to distribute the live loads through the soil fill, and project drawings were used to develop connection details in FE models. AASHTO's design truck, HL-93, and legal trucks were passed on the calibrated culvert models, and the resulting straining actions were used to estimate load rating factors. This report provides details about the methodology used in this study, field test data and 3D FE models, and load rating factors for the 8 culverts covered in this study. Finally, recommendations and research needs are presented.

17. Key Words	18. Distribution Statement
reinforced concrete; cast-in-place; culverts; bridges, live load, load rating	Unrestricted

19. Security Classification (of this report)	20. Security Classification (of this page)	21. No. of Pages	22. Price
N/A	N/A		N/A

Project Review Committee

Each research project will have an advisory committee appointed by the LTRC Director. The Project Review Committee is responsible for assisting the LTRC Administrator or Manager in the development of acceptable research problem statements, requests for proposals, review of research proposals, oversight of approved research projects, and implementation of findings.

LTRC appreciates the dedication of the following Project Review Committee Members in guiding this research study to fruition.

LTRC Manager
Walid Alaywan, Ph.D., P.E.
Senior Structures Research Engineer

Members
Arthur D'Andrea
Dana Feng
Ching Tsai
David Miller
Steven Sibley
Haylye Brown
Alden Allen
Michael Boudreaux

Directorate Implementation Sponsor
Christopher P. Knotts
DOTD Chief Engineer

Live Load Rating of Cast in Place Box Culverts

by

Ayman M. Okeil, Ph.D., P.E.(FL)
Professor

Tuna Ulger, Ph.D.
Research Associate

Ahmed Elshoura
Graduate Student

Department of Civil and Environmental Engineering
3255 Patrick F. Taylor Hall
Louisiana State University
Baton Rouge, LA 70803

LTRC Project No. 16-3ST
State Project No. DOTLT1000108

conducted for

Louisiana Department of Transportation and Development
Louisiana Transportation Research Center

July 2018

ABSTRACT

Cast-in-place (CIP) reinforced concrete (RC) box culverts constitute a large portion of Louisiana's bridge inventory. Culverts constructed using old detailing standards, especially the ones with lower fill heights, typically produce lower load rating factors when AASHTO procedures are followed. Nevertheless, the performance of these culverts is typically acceptable, and they rarely show signs of distress. The purpose of this project is to assess the load rating of representative CIP-RC box culverts from the Louisiana DOTD inventory. Eight culverts with different fill heights and pavement types were selected for the study. In the first phase of this research, field live load testing of the culverts was conducted after instrumenting each culvert with a structural health monitoring (SHM) system consisting of a total 48 sensors including displacement, strain, and tiltmeter sensors. In the second phase of the research, refined three-dimensional (3D) finite element (FE) models were built for each tested culvert and were calibrated using measured field data. AASHTO's Manual for Bridge Evaluation (MBE) rating methodology was followed in this research to distribute the live loads through the soil fill, and project drawings were used to develop connection details in FE models. AASHTO's design truck, HL-93, and legal trucks were passed on the calibrated culvert models, and the resulting straining actions were used to estimate load rating factors. This report provides details about the methodology used in this study, field test data and 3D FE models, and load rating factors for the 8 culverts covered in this study. Finally, recommendations and research needs are presented.

ACKNOWLEDGMENTS

The authors gratefully acknowledge the financial support provided by the Louisiana Transportation Research Center (LTRC) through Project No. 16-3ST. Many people helped the research team during the course of this study by providing technical input and/or field support. Their help is greatly acknowledged. Special acknowledgment is due to DOTD Bridge Design Section (P. Fossier, A. D'Andrea, Dana Feng, Ching Tsai, and Qiming Chen) for initiating the idea that led to funding this project by LTRC and for providing the available culverts data. LTRC's support extended beyond funding and managing the project and included testing concrete cores from the tested culverts. Hence, the authors greatly appreciate W. Alaywan, Project Manager, Amar Raghavendra, Concrete Testing Lab, and Tyson Rupnow for allowing this project to happen on such a short notice and tight schedule. Finally, the selected culverts that were tested in this study were geographically spread over the state, and it would not have been possible to complete this study without the help and support of DOTD personnel from the districts in which these culverts are located.

IMPLEMENTATION STATEMENT

Results from investigating the eight culverts considered in this study confirmed that following AASHTO procedures for culverts leads to conservative load rating factors, which in many cases may require owners to address the resulting factors by load posting or structural upgrading. It appears that it may not be necessary to resort to such actions since the performance and the conditions of such culverts do not indicate any structural deficiencies that warrant them. The source of conservatism in AASHTO's load rating procedure appears to be inherent in the live load distribution equations that sum all soil and structural effects into one expression. Field tests and three-dimensional (3D) models (i.e., refined models), showed that truck axle loads were resisted by a wider area than the width of the area resulting from AASHTO's equations. Refined models are capable of capturing the actual live load distribution on reinforced concrete (RC) culverts, which in the opinion of the research team should be divided into two sources, namely soil (primary) distribution and structural (secondary) distribution.

Based on this initial understanding of the behavior of RC box culverts, the following essential information can be provided to engineers involved in load rating of culverts:

1. *Model 2D-a:* Modeling of culverts using two-dimensional (2D) models should be first attempted for load rating using information extracted from standard plans and construction records. In this type of model,

    a. use beam elements representing a typical segment for modeling the culvert's slabs and walls,

    b. rigidity of the connections can be taken advantage of by introducing rigid links for distances reflecting the overlapping wall/slab regions including haunches if provided,

    c. it is necessary to introduce a hinge in the slab at the connection with the exterior walls,

    d. a rigid subgrade underneath the culvert's bottom slab, which was more conservative for the modeled culverts, should first be considered.

2. *Model 2D-b:* If Model 2D-a does not produce acceptable loading factors; the engineer should attempt to:

    a. introduce axial springs underneath the culvert to represent the soil subgrade,

b. the stiffness of the springs should be determined based on the actual soil conditions at the site of the culvert,

c. alternatively, a value of 150 pci for the modulus of subgrade reaction, which for a medium soil mixture consisting of sand/clay/silt, was used due to the lack of more accurate information.

d. Other aspects of the model should be kept identical to those described for Model 2D-a.

3. *Other 2D Modeling Improvements:* In the case that a 2D model still does not produce acceptable loading factors, the following measures could be tried:

    a. Obtain actual concrete strengths through coring. Concrete compressive strength is known to increase overtime. Furthermore, many contractors target an initial concrete strength higher than what is specified for a certain project to avoid rejection if a batch does not meet the specs. This was the case for all eight tested culverts and such an increase can help improve rating factors. Alternatively, increase in concrete strength over time may be taken advantage of using established formulas in the literature (e.g., ACI 209 Report).

    b. If modeling a culvert using *Model 2D-a* or *Model 2D-b* in a software package such as BrR that does not allow the introduction of rigid connections, and the results show that the exterior wall controls the load rating, the effect of horizontal earth pressure (EH) and surcharge (ES) can be reduced using hand calculations following the procedure proposed in this study or charts similar to the ones presented in this report. Similar procedures can also be used for reducing the applied loads on the top slab by taking advantage of the rigid connections, however, the reduction will have to be determined on a case by case basis.

4. *Model 3D:* If both 2D models (Model 2D-a and Model 2D-b) do not result in acceptable load rating factors, a three-dimensional model should be attempted. For the 3D model:

    a. shell elements should be used for the culverts slabs and walls instead of the beam elements used in 2D models.

    b. rigidity of the connections should be taken advantage of by introducing rigid links for distances reflecting the overlapping wall/slab regions including

haunches if provided,

c. a hinge reflecting the lack of negative moment reinforcement in the slab at the connection with the exterior walls should be introduced,

d. a rigid subgrade underneath the culvert's bottom slab appears to be adequate for capturing the actual behavior observed in the field.

5. *Other 3D Modeling Improvements:* In the case that a 3D model still does not produce acceptable loading factors, the following measures could be tried:

    a. Obtain actual concrete strengths through coring or use established formulas from the literature as stated earlier (See 3-b).

    b. Conduct live load tests as a last resort. Field tests reflect the actual behavior of the structure taking into accounts its actual ability to distribute the loads and the interaction between the structure and the surrounding soil. Calibrating 3D models using field test data improves the accuracy of the model, which would improve the load rating of the culvert.

Load rating factors using this model should be calculated for design and legal trucks as per LA BDEM using AASHTO's distribution equations.

TABLE OF CONTENTS

LIST OF TABLES

LIST OF FIGURES

INTRODUCTION

This report provides detailed investigation of eight cast-in-place (CIP) reinforced concrete (RC) box culverts from DOTD's inventory. The eight selected CIP- RC box culverts are representatives of thousands of Louisiana culverts with low fill heights. They were selected by the DOTD Bridge Design section for this study and were load tested by the research team from Louisiana State University. The purpose of field testing was to investigate the behavior of these culverts and their load rating performance as it is known that conventional AASHTO load rating methods often result in unacceptable low rating factors, which may require action to address such an outcome. Understanding the behavior of CIP-RC box culverts and its relation with load rating provides the basis for developing a new rating methodology that can be used for Louisiana culverts built according to the old standard details. It will also identify and highlight the research needs for addressing the long-term goal of assisting in load rating all of the culverts in DOTD's inventory.

Load Rating of Culverts

According to the National Bridge Inventory (NBI), Louisiana has approximately 2,600 culverts. Buried cast-in-place reinforced concrete culverts are known be a robust structural system that can withstand highway traffic because they behave as a highly static indeterminate system. The design of culverts differs from other types of bridges. First, single axle loads, and sometimes single wheel loads, are the controlling live load conditions for the design of culverts, as opposed to the gross vehicle weight (GVW) that controls the design of typical bridge spans. Second, the depth of the soil fill above any culvert is determined based on the hydraulics and roadway geometric conditions at the bridge site, which is known to vary greatly and accordingly has a great impact on the live load effects on the buried culvert. In 2010, National Cooperative Highway Research Program (NCHRP) Project 15-29 produced Report 647 "Recommended Design Specifications for Live Load Distribution to Buried Structures" *[1]*. Simplified design equations (SDEs) for the structural response of buried structures based on three-dimensional (3D) analysis of 830 buried culverts were developed. The report also provides guidelines for conducting 2D and 3D modeling analyses for culverts that are not covered by the SDEs. In this work, the effect of pavement on live load distribution was ignored, which can have a significant effect on reducing actual pressures that reach the box. While this may be a conservative assumption for design purposes, it penalizes existing culverts with rigid pavements over their top soil fill as can be seen in Figure 1 obtained from a publication by the American Concrete Pipe Association in 2007 *[2]*.

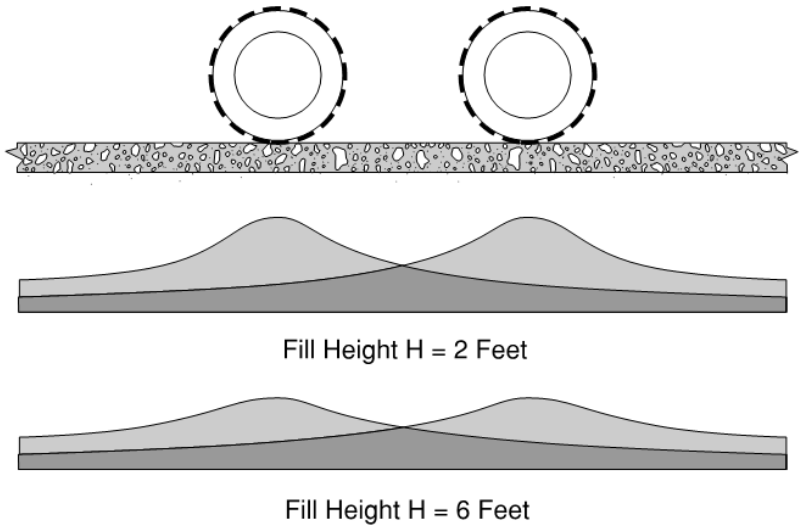

Figure 1
Effect of pavement on wheel load distribution *[2]*

Live load effects from highway trucks are often simply assumed to spread as a surface load over an area whose dimensions can be determined based on a linear function of depth. Acceptable designs have been produced based on this approximation method for estimating the distribution of vehicular live loads through earth fill AASHTO Standard Specifications or Load Factor Design (LFD) *[3]*. Figure 2 shows a schematic of how live load pressures spread from the surface where the pressure is spread of the tire contact area (typically 10 in. x 20 in.) to a larger area at a given depth, *H*. Three cases are shown representing: (a) the case of a single wheel load, (b) the case of two single wheel loads from adjacent trucks in a passing mode, and (c) the case of two axles of the case described in (b). The current AASHTO Bridge Design Specifications, which is based on the Load and Resistance Factor Design (LRFD) methodology, adopted a different approach that led to increases in live load pressures on buried structures *[4]*. This is further exacerbated by the higher dynamic allowance in AASHTO LRFD.

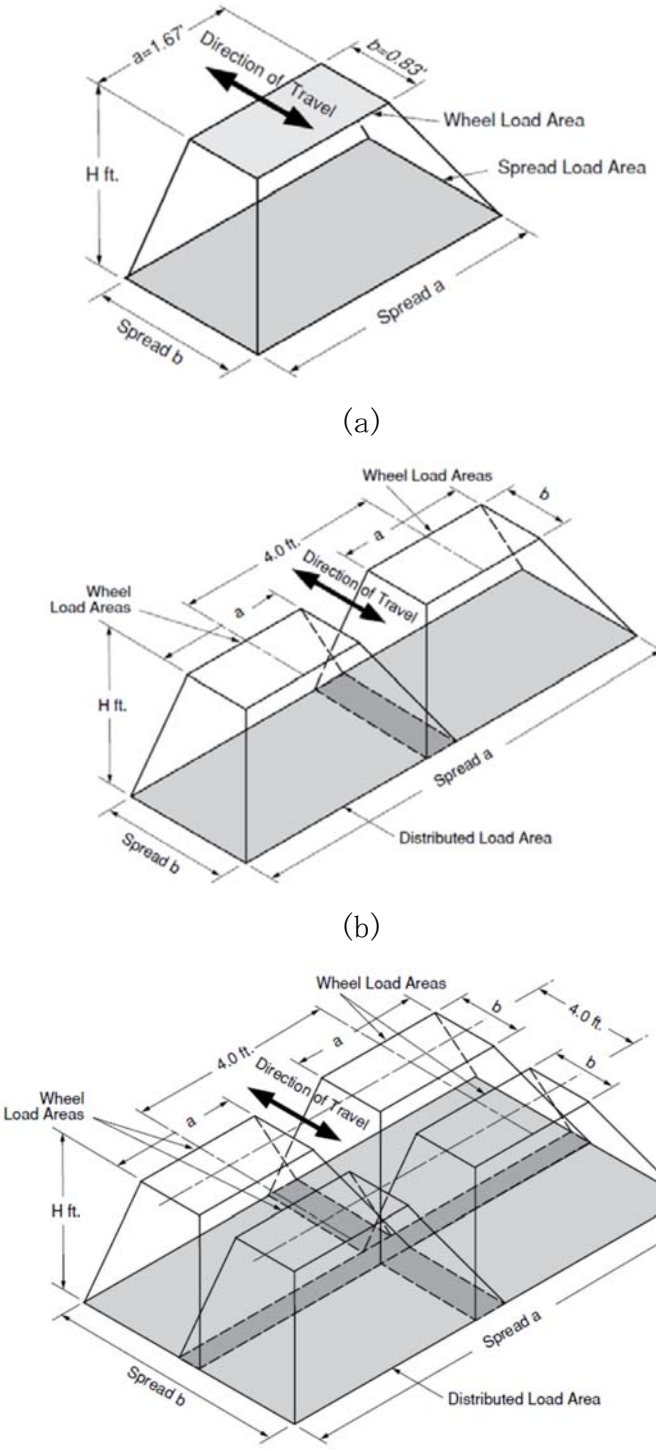

Figure 2
Area of live load distribution – (a) single wheel (b) two single wheels in passing mode (c) two axles of two single wheels in passing mode *[2].*

Reinforcement detailing also has its implications on reinforced concrete box culvert rating. Multicell structural systems are highly statically indeterminate, and therefore are capable of resisting larger pressures than similar ones with lesser degrees of indeterminacy. However, the degree of indeterminacy of multicell box culverts may be reduced if the reinforcement detailing at the corners is not capable of transferring internal forces produced in such systems. Many of the RC-CIP box culverts in Louisiana's were built with old details that may fall under this category. Figure 3 shows one of these details, which reveals that: (1) exterior wall reinforcement is not adequately embedded in the top or bottom slabs of the box, (2) a single layer of reinforcement in these walls and at the ends of the top and bottom slabs make them incapable of resisting negative moments that would generate in a fully rigid corner joint. Engineers have typically considered these connections to behave like hinges rather than rigid connections.

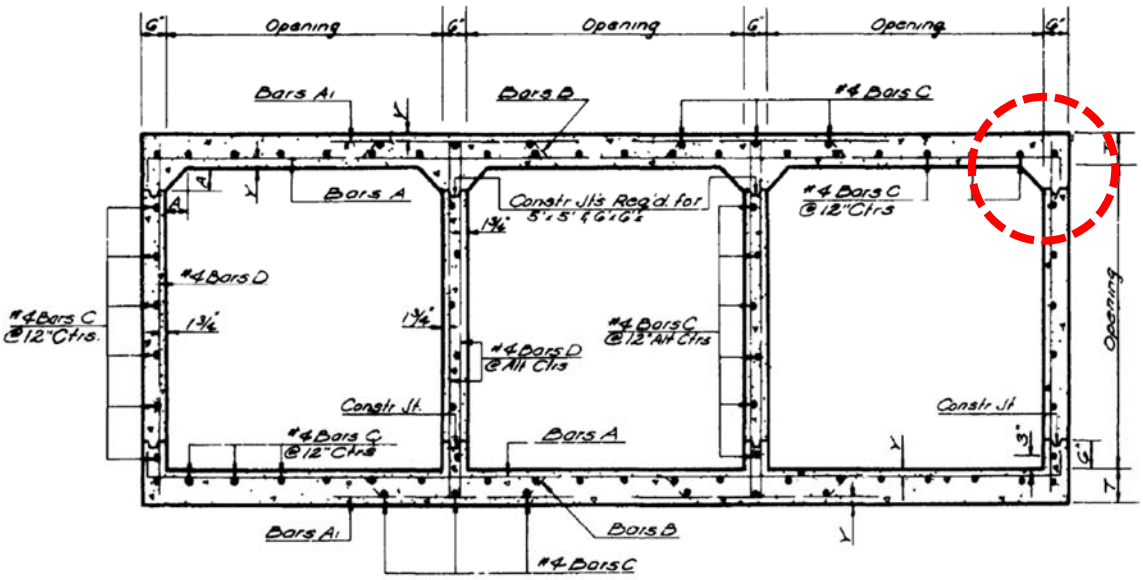

Figure 3
Old DOTD standard detail for a three-cell CIP box culvert

The conventional approach for load rating CIP-RC box culverts relies on only available project data and assumptions without considering the real structural performance of the culvert. Consequently, assumptions are usually made to reflect the plans for the constructed culvert project. As stated earlier, hinges are often assumed at wall slab connections (see Figure 3) to reflect the lack of negative reinforcement required to resist moments that would develop if a rigid connection is assumed instead. Similarly, material properties are typically extracted from the project records, which ignores any increase in concrete strength that is known to take place over time. Furthermore, these assumptions are often incorporated in

two-dimensional (2D) finite element (FE) models, which are also know to add to the conservatism of the load rating process.

FE models can be based on simple frame elements (2D models) to the more complex 3D models including all surrounding soil-structure interaction using more advanced brick elements. After extensive literature reviews, the authors agreed to use 3D models such that the inherent conservatism introduced by 2D models is eliminated and a closer behavior to the actual culverts could be obtained. Some of the research on live load distribution is presented in the next section to highlight the spectrum of available models; each with its advantages and limitations.

Live Load Distribution on Concrete Box Culvert

In addition to gravity loads (e.g., self-weight, earth fill, wearing surface, etc.) that affect the design and rating of culverts, live loads which are distributed at the top slab of the culvert also have to be considered. While gravity loads are typically uniformly distributed over the culvert's top slab, live loads are not. The intensity of wheel loads is attenuated through the pavement layers, embankment soil, and the top slab of the culvert. Live load distribution is affected by several factors that many researchers have investigated over the years. The following are a few of such efforts that highlight the importance and lack of consensus on how live load distribution should be conducted.

Abdel-Karim et al. investigated the wheel load attenuation through each of the aforementioned stages (pavement layers, embankment soil, and top slab) *[5]*. The researchers conducted a live load test on a culvert with different fill height ranging from 2 ft. to 12 ft. (above the top slab of the culvert) and the pressure on the surface of the structure was measured using pressure cells. In general, it was found that the wheel load is distributed over a square area, but by increasing the fill height, the distribution becomes more uniformly in a larger area with lower peaks except for 2 ft. fill height. Moreover, the rigidity of rigid pavement was shown to help distributing the live load in a larger area because of its higher flexural rigidity. The study introduced a method for calculating an additional width to reflect the existence of rigid pavement by converting the pavement thickness into an equivalent fill height. Such additional distribution can be neglected for flexible pavement. It was also noted that the wheel load will be dispersed over a larger area due to the flexural rigidity of the culvert top slab.

McGrath et al. studied the live load distributions for fill height less than or equal to 2 ft., and made a comparison between AASHTO Standard specifications and AASHTO LRFD specifications *[6]*. The study found that LRFD specifications give more conservative forces

effects, for box culverts with span lengths of 15 ft. or less, whereas less conservative forces effects results using the AASHTO standard specifications. Furthermore, the study concluded that the live load distribution width for shear forces is smaller than the positive moment distribution width for culvert design.

The shear behavior of precast reinforced concrete culverts was investigated experimentally by Abolmaali and Garg *[7]*. Six full-scale (8-ft.) culverts were tested in the lab up to failure under a simulated wheel load applied at different distances along the span length. The experimental results showed that flexure governed the behavior well beyond the calculate AASHTO factored loads. Shear cracks only formed after exceeding twice AASHTO's calculated factored load indicating that the culvert's shear strength is than that obtained using AASHTO provisions. The authors also concluded that the AASHTO's load distribution is not representative of the culvert's behavior and should be revisited.

Orton et al. published results from testing ten reinforced concrete culverts with fill depths ranging from 2.5 to 13.5 ft. with the objective of determining the effects of live loads on culvert behavior *[8]*. By comparing measured and calculated strains and displacements, the authors concluded that AASHTO-LRFD specifications is overly conservative. It was also concluded that the live load effect can be ignored for fill depths exceeding 6 ft.

Wood et al. conducted a study to assess the live-load rating of three culverts with different earth-fill height, dimensions, and spans. In the study, two finite element (FE) models are used to study each culvert *[9]*. The first model is a 2D model that uses structural-frame elements for the various culvert components (walls and slabs). and a 2D soil-structural interaction model which are calibrated with live load tests. The goal was to figure out the difference in accuracy and precision between the two models results from the live load distribution. The measured moment, from LL test, at each case was compared with the predicted ones from the models. In 2D frame element models, live loads were distributed according to AASHTO specifications, whereas the axel-loads were dissipated depending on the soil mesh in the 2D soil-structure interaction. The research come up with both models are conservative, however the 2D soil-structure interaction was found to be more precise. Furthermore, the accuracy of both models improved by increasing the soil fill depth, however, the precision varied for different critical sections, i.e. the predicted moments for top slab critical sections are more accurate than those for the bottom slab.

Another study done by Wood et al. discussed the accuracy and precision of live load attenuation on reinforced concrete box culverts *[10]*. It focused on a comparison between three -simplified models; namely, structural-frame model, top-slab calibrated soil-structure

model, and fully depth-calibrated soil-structure model. In the first model, the soil is considered as a dead load only and it attenuates the wheel (concentrated) live load as recommended in AASHTO's Manual for Bridge Evaluation (MBE). In the MBE, the pressure on the culverts top slab equal to wheel load, P, divided by the area defined by the influence area in the out-of-plane and in-plane directions ($W L$). It was found that this model overestimates the culvert's rating factor for culverts. For the second model (i.e., top-slab calibrated soil-structure model), a line load is applied at the ground surface, and it is distributed to the walls, top slab, and the bottom slab of the culvert, i.e. to the critical sections. The intensity of line load is the wheel load divided by the effective live-load width. It was found that this model gives a more accurate load rating factor as it distributes the stresses at the bottom slab, and captures the structural response better than first model. The last model, fully depth-calibrated soil-structure model was found to distribute the live-load differently according to the studied critical section. In other words, the value of line load applied at the ground surface depends on the position of the critical section. The authors concluded that this model results in the most accurate and precise load factor.

Acharya et al. studied the influence of concrete pavement layer and span length on the live-load distribution over culverts *[11]*. The study found that the presence of pavement increases the rating of a culvert because it helps distributing the live-load over a wider area. It was found that the intensity of distributed pressure increases with the decrease in span length, especially for low fill height. Furthermore, the thicker top slab thickness is, the more pressure act on the culvert.

In another study by Acharya et al., a reinforced concrete box culvert with low-fill was tested under static and moving live load *[12]*. The research aimed at understanding the effect of vehicle axle-load, its speed, and pavement structure on the roof of buried culvert and corresponding deflection. The test was run under a static load at three different locations; namely, concrete pavement, concrete shoulder with a thinner concrete pavement, and unsurfaced area. An additional live load dynamic test (moving load) was also performed, however, only at the location under the paved concrete section of the roadway. Field test data showed that the top slab deflections over the unsurfaced area due to the static load were 2-3 times higher than deflections under the concrete pavement and concrete shoulder as a result of the stiffness of the concrete pavement, which assists in distributing wheel loads over a larger area, lowering pressure intensity. It was also observed that the moving load created larger deflections than static loads.

Frederick and Tarhini conducted a study to evaluate the design of precast reinforced concrete box culverts complying with ASTM Specifications C789 and C850 using AASHTO live load

distribution provisions *[13]*. The experimental program employed 1/6-size scale models and 1/24-size photoelastic model of three culvert prototypes with different dimensions. By comparing the strains and deflections resulted from the model test and field test results of the culvert prototypes, the authors noted that AASHTO live load distribution equation is conservative, and that the live load is dissipated over a wider area. It was concluded that culverts design according to ASTM C850 were over-designed.

Earlier Research on Culverts in Louisiana

The Louisiana Transportation Research Center funded several studies on buried culverts in the past. However, the work was mainly focused on metal culverts *[14-16]*. The lightweight and flexibility of metal pipes makes them an appealing alternative to other types of culverts. However, their susceptibility to corrosion is a disadvantage. The effort was started in 1977 to study the durability of buried metal pipe culvert was initiated to address corrosion of metal pipe culverts in the highly corrosive environments in which they are typically employed. This initiated the motivation for inspecting six different types of existing culvert metal pipes and another four new types to evaluate the rate and causes of corrosion and durability. The authors observed that asbestos-bonded asphalt-coated galvanized steel culverts performed better than other types of culverts considered in the study after 6 years of in-service monitoring.

Several reports were published in the 1990s on coated metal pipe culverts *[17-19]*. The main focus of these studies was to investigate the feasibility of cathodic protection both externally and internally to prevent corrosion in corrugated steel pipes, hence, reducing the costs of having to maintain or replace this type of culverts. In this research, cathodic protection was applied to retrofitted metal pipe externally and internally and monitored for two years. The same protection process was applied on a new metal pipe culvert and monitored for one year. The monitoring results indicated that cathodic was very effective for an existing pipe externally but not for internal protection. However, cathodic protection was effective for internal and external corrosion protection for new culverts. The information from monitoring was used to develop a computer expert system software to assist designers in assessing the economics of employing cathodic protection systems in metal culverts in Louisiana.

Performance of Louisiana's RC-CIP Box Culverts

In general, the real performance of low rated Louisiana culverts contradicts the AASHTO load rating calculations despite their age and lack of reinforcing bars in negative moment corner details. This is based on visual inspection of the eight culverts and on discussions with engineers involved in culvert load rating in Louisiana and elsewhere. For the culverts

covered by this study, the lack of structural cracking due to higher moments, excessive deflections, deterioration of concrete quality, and corrosion of reinforcement were indications that the culverts were operating well and capable of carrying the roadway traffic to which they are subjected. It should be noted cracks were observed for some culverts, however, these cracks were mainly caused by differential settlement due to scour around the culverts ends.

Research Needs

As can be seen from the brief review of published efforts on live load rating of reinforced concrete box culverts, there is no consensus on how live loads should be distributed for design and load rating purposes. There is a consensus, however, on the fact that current provisions pose a challenge to bridge owners as they produce conservative assessments that sometimes lead to insufficient load rating factors. Consequently, action is typically required from bridge owners to address the low rating factors. Thus imposing an additional strain on the limited available resources.

The immediate research need for culvert load rating is to provide a methodology for dealing with CIP-RC box culverts in the DOTD's inventory that were built using old standard details. The developed methodology will be complemented with field live load testing for a select few culverts from DOTD inventory to better understand the actual behavior of CIP-RC box culverts in service. The long-term need in Louisiana, and the entire nation, is to fully understand the different factors that affect live load distribution such as fill height, pavement type, soil type, and culvert's structural and geometric characteristics. A comprehensive methodology that could assist engineers in designing and load rating CIP-RC box culverts without introducing unnecessary conservatism is the ultimate goal of this project.

This study looks into the short term need as a first step towards addressing the long-term needs. It will help DOTD by: (1) understanding the behavior of the eight culverts considered in this study, (2) comparing load rating results that are based on field load testing and calibrated 3D FE models to traditional methods to develop an understanding of the scope of limitation on traditional load rating method

OBJECTIVE

The main objective of this study was to assess live load effects on eight cast-in-place (CIP) reinforced concrete (RC) box culverts by conducting field load tests. These culverts were selected by the DOTD Bridge Design Section and were instrumented to monitor their response to live load effects. Understanding the actual response of the culverts will provide insight as to how the live loads are actually distributed as well as the actual rigidity of the box corner connections.

The goals of this project were to:

1. Study the current standard DOTD's culvert drawings and the inspection reports for the eight selected culverts.
2. Define critical sections and produce culvert specific instrumentation plans.
3. Instrument the culverts by installing the sensors at specified locations and evaluate the current condition.
4. Conduct the live load test and collect sensor data.
5. Build FE models for each culvert and calibrate them using collected sensor data.
6. Load rate the selected culverts for design and legal trucks.
7. Provide the rating details and recommendations to assist rating of CIP-RC box culverts.

SCOPE

This study focused on live load rating of eight cast-in-place (CIP) reinforced concrete box culverts from DOTD's inventory. The fill heights over the selected culverts varied but were chosen to be mostly with low soil fill since this condition is known to pose rating challenges. A structural health monitoring (SHM) approach was adopted for assessing the actual performance of the selected culverts. The SHM system employed three different sensor types to instrument the top slab and wall sections in one exterior and one adjacent interior openings. Experimentally obtained sensor data under known truck loading provided the actual structural behavior of CIP. Three-dimensional (3D) FE models were developed based on the provided and measured properties of the culverts and calibrated using field load test response measurements to determine refined live load rating factors considering HL-93 design truck and 10 different legal trucks.

The results and findings from this investigation will provide detailed FE modelling and rating methodology for the selected eight CIP culverts, which are described in the next section.

METHODOLOGY

Selected Culverts

The culverts considered in this study were selected by DOTD from the department's vast inventory of over 2,500 culverts that qualify as bridges, having a span length of 20 feet or longer. The main criteria used in selecting the culverts were: to be built as a CIP-RC box structure and to have a low soil fill on top of it. Figure 4 shows the locations of the culverts covered in this study, which was geographically scattered all over the state. It should be noted that the research team visited more culverts than is listed in this report. However, the other inspected culverts did not fit within the scope of the study (e.g., precast concrete), and, hence, were excluded.

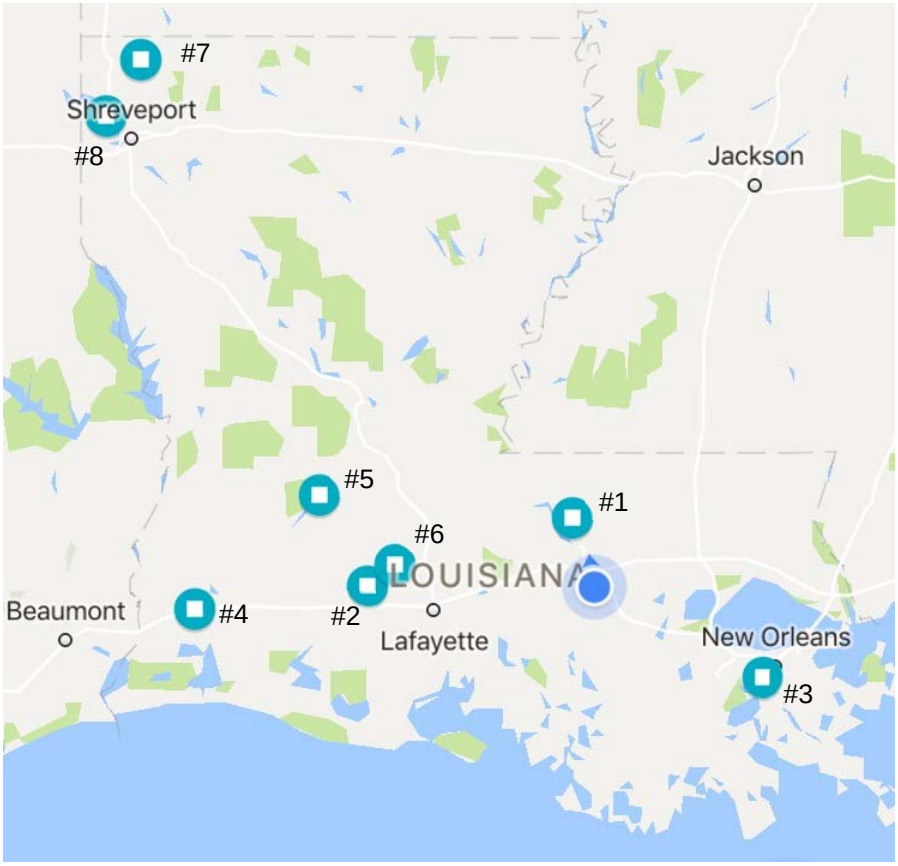

Figure 4
Locations of final eight culverts included in this study

The latest inspection report and standard plans for each culvert were provided to the project team before the field tests to extract dimensions and other details necessary for planning each test and setting an appropriate instrumentation plan. The roadway over only two of 8 tested culverts had rigid concrete pavements and the rest had asphalt pavements. Three of the tested

culverts were skewed. The other five culverts were not skewed, except for Culvert #3 whose skew angle (86.7°) was practically perpendicular to the road. Fill heights were measured by DOTD during the test day and provided to the research team for inclusion in the model. In general, fill heights ranged between 13 in. and 7 ft. for the selected culverts. Concrete samples were cored out of the walls of the tested culverts and tested by LTRC Concrete Material Lab. The results from the core samples were provided to the research team later in the project. The locations of the tested culverts and the relevant routes are given in Table 1. Table 2 lists the traffic and main geometric characteristics of the tested culverts as well as the dates on which they were tested. It also lists the fill heights, which were determined from surveys undertaken on the day of load testing.

Table 1
Tested culverts location

Culvert #	Location	Recall	Structure #	Location (LAT/LONG)	Route	Year Built
1	Zachary	610033	P173050911281	30.683300 –91.230583	Plains-Port Hudson Rd	1957
2	Crowley	003910	3010570309911	30.348276 –92.397601	LA 13	1960
3	New Orleans	020299	2262830907131	29.898338 –90.142765	US 90	1992
4	Sulphur	031410	7100030312721	30.236565 –93.384425	US 90	1967
5	Oakdale	070210	7020140412911	30.723971 –92.711022	US 165	1980
6	Church Point	008310	3498490502781	30.454698 –92.244510	LA 751	1970
7	Plain Dealing	012580		32.906533 –93.698381	LA 2	1959
8	Blanchard	013960	4090450106901	32.635494 –93.893828	LA 1	1939

Table 2
Tested culverts traffic, geometric characteristics and test dates

Culvert #	ADT	Opening Size (ft. x ft.)	Number of Openings	Skew Angle (°)	W.S.	FH (ft.)	Test Date
1	931	7 x 7	4	90	A	2.20	09/28/2016
2	5,200	6 x 6	5	90	A	7.00	11/16/2016
3	63,200	8 x 8	3	86.7	A	1.08	12/17/2016
4	10,500	12 x 12	2	90	A	2.24	03/09/2017
5	10,476	7 x 7	3	45	C	4.14	03/23/2017
6	830	5 x 4	3	45	A	1.78	03/28/2017
7		6 x 6	3	60	C	1.08	05/10/2017
8	7,000	8 x 8	4	90	A	1.60	05/11/2017

W.S. = Wearing Surface, A = Asphalt pavement, C = Concrete pavement, FH = Fill Height

The available project data was used to design an instrumentation plan that is capable of capturing the behavior of the tested culverts in an exterior barrel and one adjacent interior barrel. The provided data, including the experimentally obtained concrete properties, was also directly used in FE modelling and model calibration as will be described later. Table 3 lists the additional information about the selected culverts. The wall and slab thicknesses were extracted from the provided plans and confirmed from site inspection. Concrete compressive strength, f_c', was determined by testing core samples from culvert walls, which was consistently higher than the values extracted from the construction plans. The remaining columns in Table 3 list the load values considered in culvert design and load rating. They were determined based on the listed dimensions. It should be noted that when needed to calibrate the FE model sensor readings, the considered slab thickness was increased by about 10-15% to consider the possible thickness variation of slab sections during construction.

Table 3
Culvert properties and effective dead loads and live surcharge load

Culvert #	Slab / Wall Thickness (in. /in.)	f_c' (psi)*	E_s (ksi)	DW (ksf)	EV (ksf)	EH (ksf)		ES (ksf)	LS (ksf)
						Top	Bot.		
1	8.5 / 7.0	6,326	29,000	0.070	0.206	0.144	0.683	0.035	0.176
2	8.0 / 6.0	6,693	29,000	0.070	0.811	0.410	0.810	0.035	0.154
3	9.0 / 8.0	8,948	29,000	0.070	0.070	0.057	0.582	0.035	0.177
4	12.0/ 12.0	8,971	29,000	0.070	0.211	0.134	0.914	0.035	0.143
5	8.5/ 7.0	10,662	29,000	0.121	0.408	0.221	0.686	0.060	0.164
6	7.5 / 6.0	9,018	29,000	0.070	0.156	0.096	0.373	0.035	0.216
7	8.0 / 6.0	9,268	29,000	0.070	0.070	0.066	0.550	0.036	0.199
8	9.0/ 8.0	7,158	29,000	0.070	0.133	0.103	0.716	0.035	0.173

* obtained from testing core specimens

SHM System and Instrumentation Plans

In this project, a Structural Health Monitoring (SHM) system comprising of three different sensor groups was employed to obtain field data. The total number of the sensors in the chosen SHM system was 48, all of which were surface-mounted. The breakup of these sensors was as follows: 36 strain sensors, 8 Linear Variable Differential Transducers (LVDTs), and 4 tiltmeters. For culverts under a perpendicular roadway; i.e., 90^o skew, strain sensors were bonded perpendicular to the wall which is also parallel to the traffic direction, and the maximum strain resultant was directly obtained during the field test. For skewed culverts; i.e., skew angle less than 90^o, sensors were still placed perpendicular to the wall, which is the shortest path for applied wheel loads. In this case, the traffic did not travel in the sensor direction. As such, the field results are obtained for the maximum strain resultant for all the culverts (skewed and non-skewed) avoiding the need to perform post-processing to obtain maximum strain readings. Furthermore, this sensor orientation reduces calibration error because the reading values are larger than those that would have been obtained had the sensors were placed parallel to the traffic direction. Strain sensors used for this study originally manufactured and calibrated as 3-in. gauge length. However, it is always recommended for concrete structures to have a longer gauge length to avoid stress localization issues resulting from cracking of lack of homogeneity. Therefore, a linear

extension was added to the original sensor length as recommended by the manufacturer to increase the gauge length by 3 in. Culvert #1 was instrumented using sensors with and without extensions to test the performance of the sensors, and there was not any significant difference in magnitude of strain readings from neighboring sensors. The other culverts were instrumented with strain sensors using linear 3-in. extension, thus creating a 6-in. gauge length. Since the original sensors were calibrated for their original gauge length, L_i, a correction factor had to be introduced for the extended sensors using the formula given in equation (1). It should be noted that the recorded readings the tested culverts imply that the culvert slabs are not structurally cracked (few cracks were observed because of bad workmanship or soil settlement close to culvert ends). This explains the similarity of readings obtained using sensors with and without extensions.

$$\psi_s = \frac{1}{0.9 * \left(\frac{L_{ext}}{L_i}\right)} \quad (1)$$

where,

ψ_s = sensor data correction factor for extended strain gauges

L_i = original strain gauge length (3 in.) without extension

L_{ext} = total extended length ψ_s

Strain sensors were placed at mid-span and at corner locations of top slab/wall connections. A clear 6 in. distance was provided from the end of the haunch so that installation and disassembling of the sensors could be completed easily. A typical sensor plan is shown in Figure 5, which shows three different truck load paths that were typically used in this study. The positions of the sensors inside the two instrumented barrels (one exterior and one adjacent interior) can be seen in the cross-sectional detail view shown in Figure 6. In the figure, four tilt-meters and one mid-span LDVT can be seen in addition to the strain sensors. Six other LVDTs were installed across the exterior barrel of the culvert to capture the deformation of the box under all three load paths. The eighth LVDT was installed in the adjacent interior barrel to complement the readings for one of the load paths; Load Path 2 in the shown plan. The specific instrumentation plan for each of the eight tested culverts is provided in Appendix A.

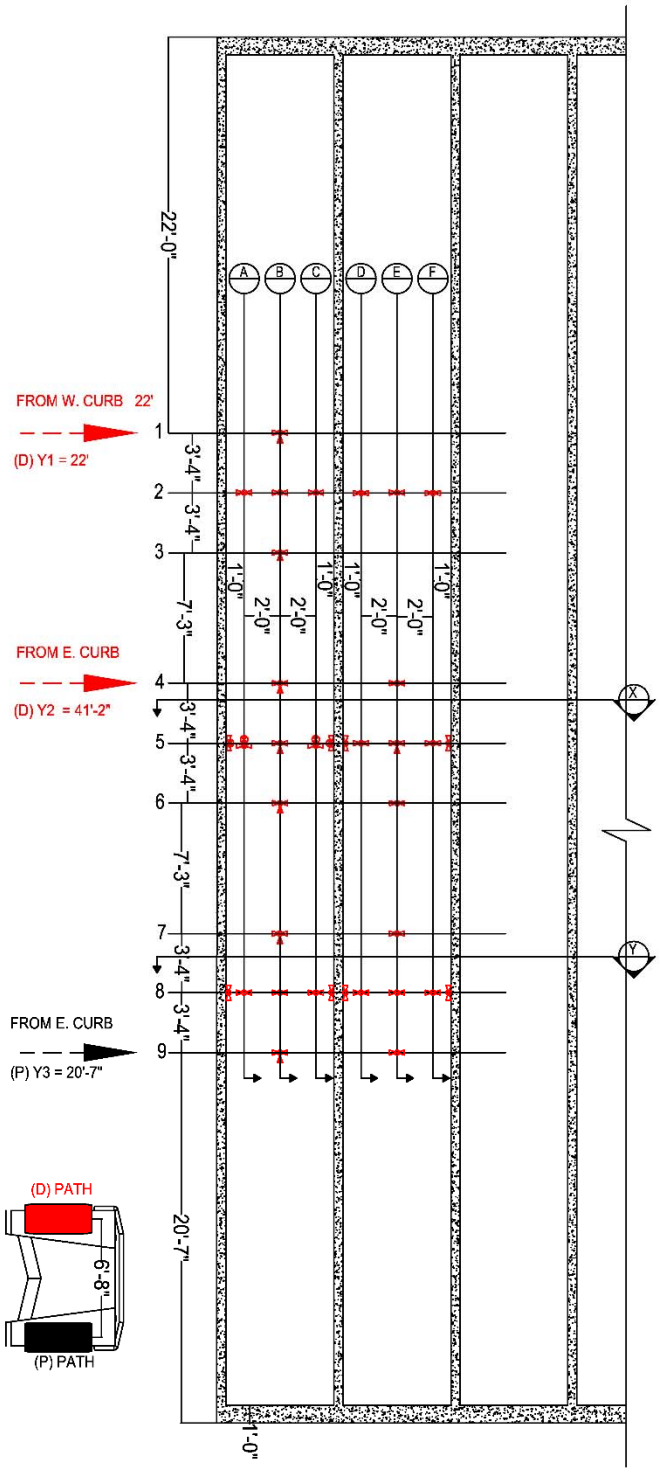

Figure 5
Typical sensor instrumentation plan

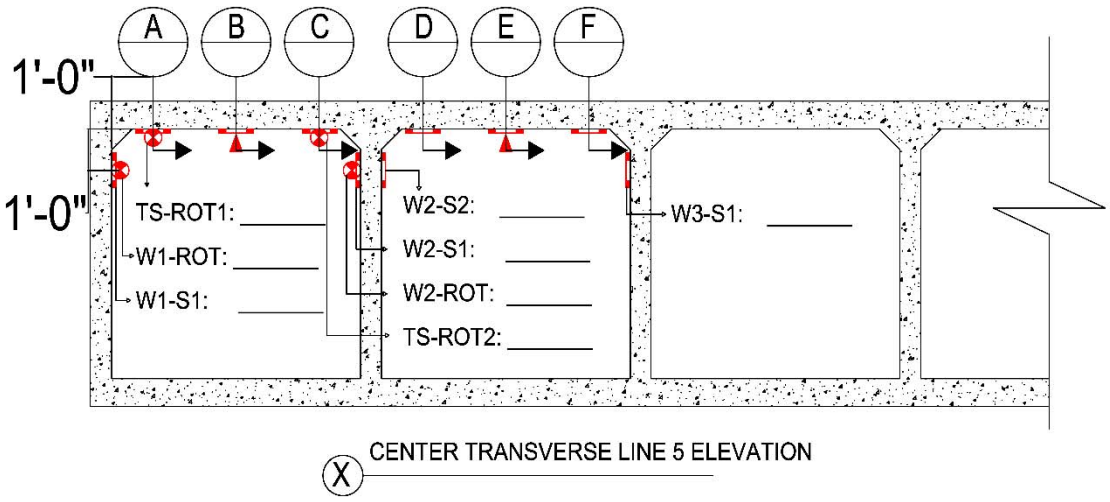

Figure 6
Typical sensor positions in a culvert

Rating Methodology

In this section, the methodology followed in load rating the culverts covered in this study is presented. The real structural response of the buried CIP-RC box culverts due to pre measured truck live loads were extracted using strain, displacement and tiltmeter sensors. The field data served as a calibration input for three-dimensional (3D) finite element (FE) models developed as part of this study for each culvert. The live load rating trucks were then passed on the culvert 3D FE models. Results from the analyses of the 3D FE models with the load rating trucks were used to extract the maximum demands they produce. Finally, the rating factors at different sections were calculated.

Permanent Dead Loads: DC and DW

Component dead loads (DC) were obtained using the sectional properties defined in the 3D FE model. The density of reinforced concrete γ_c was assumed to be 0.145 kcf for the all eight culverts. Two different types of wearing surfaces exist in this study. The wearing surface thickness was not measured during field test; therefore, the thicknesses of asphalt and concrete pavements were assumed 6 in. and 12 in., respectively. It was assumed that the density of the asphalt and concrete pavement was 0.14 kcf and 0.145 kcf, respectively.

Earth Loads: EV, EH, and ES

The road profile was surveyed relative to top of the headwalls. The height of the headwall was determined from the standard plans corresponding to each culvert; typically, 2 ft., which

typically includes the top slab thickness. From this information, the fill height was calculated as the distance from the pavement surface to top slab surface elevation. A soil density of 0.12 kcf was assumed for all considered culverts. It should be noted that the effect of wearing surface cross slope was neglected in calculation of the earth loads and live load distributions. AASHTO's simplified approach for accounting for soil-structure interaction was used by modifying the vertical earth pressure, EV, using AASHTO LRFD 12.11.2.2.1 *[3]*.

Lateral earth pressure (EH) was applied linearly proportional to the depth of the backfill soil. The coefficient of at-rest lateral earth pressure (k_o) was taken equal to 0.5 as per AASHTO LRFD 3.11.5.2 *[4]*. The pressures are reduced 50% and included with a load factor equal to 1.0 in live load rating calculations.

Uniform surcharge load (ES) defined in AASHTO MBE 6A.5.12.10.2c was also included in addition to the lateral earth pressure *[20]*. Similar to the EH, the uniform pressure value is reduced 50% and combined with load factor 1 in live load rating calculations.

Vehicular and Surcharge Live Loads: LS and LL

In this study, the HL-93 design truck and DOTD legal trucks listed in Table 4 were considered. The axle load effects of these trucks were passed on the culvert models. The straining actions (bending moments, shear forces, and axial forces) were obtained at critical sections and the rating factors for each truck are studied. The axle loads were uniformly distributed over an influence area on the top slab in FE model according to AASHTO provisions.

The effect of traffic load on the backfill was also treated as a uniform live surcharge load (LS) per AASHTO MBE 6A.5.12.10.3c *[20]*. A constant uniform pressure applied to the exterior wall surfaces. The effect of surcharge load with its load factors were included in calculation of rating factor.

Table 4
Load rating truck types and gross vehicle weights

Vehicle Type	GVW (kips)
HL-93 (INV)	N/A*
HL-93 (OPR)	N/A*
LA Type 3	41.0
LA Type 3S2	73.0
Type 3-3	80.0
LA Type 6	80.0
LA Type 8	88.0
NRL	80.0
SU4	54.0
SU5	62.0
SU6	69.5
SU7	77.5

** depends on span length*

Live Load Distribution

As stated earlier, a field survey of each culvert was conducted to determine the fill height, which is essential for calculating the dead load and distributed truck axle loads on the culvert. After the research team received the surface elevations from DOTD surveys, an approximate fill height was calculated from culvert dimensions as given in the standard plans, which were verified by field measurements whenever possible. The roadway shoulder was excluded when the approximate fill height was determined. It should be noted that as a result of approximating the fill height and to the existence of the roadway's cross slope, the center of travelling path was modeled with less fill height than the actual fill height. Conversely, the opposite is also true for the edge and shoulders.

The average fill height was used to calculate the area influenced by each truck's axle load as per AASHTO LRFD Section 4.6.2.10 equivalent strip method for fill height less than 2 ft., and Section 3.6.1.2.6 Distribution of wheel loads through earth fills for fill height equal to or greater than 2 ft. *[4]*.

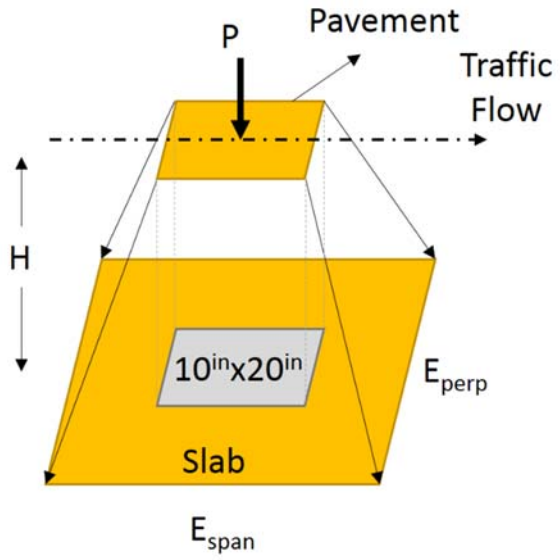

Figure 7
AASHTO live load distrubution with soil depth

The relevant equations for these two conditions are:

for $H \leq 2$ ft.
$E_{perp} = 96 + 1.44\ S$
$E_{span} = L_T + LLDF\ x\ H$ (2)

For $H > 2$ ft.
$E_{perp} = 10 + LLDF\ x\ H$ (3)
$E_{span} = 20 + LLDF\ x\ H$

where,
LLDF = factor for distribution of live load with depth of fill
H = depth of fill from top of culvert to top of pavement (in.)
S = clear span (ft.)
E_{span} = equivalent distribution length parallel to span (in.)
E_{perp} = equivalent distribution width perpendicular to span (in.)
L_T = length of tire contact area parallel to span (in.)

These equations determined the extents of the area that the soil distributes axle loads pressure on the top slab of the culverts. Depending on the fill depth, the effect of the axle's two wheels can result in two separate pressure areas (see Figure 8) or one overlapping area of pressure (see Figure 9). Skewed culverts introduce additional challenge in identifying the top

slab area affected by the wheel load pressures. Figure 10 shows one of these culverts with the load pressure from three axles as the pass over the culvert.

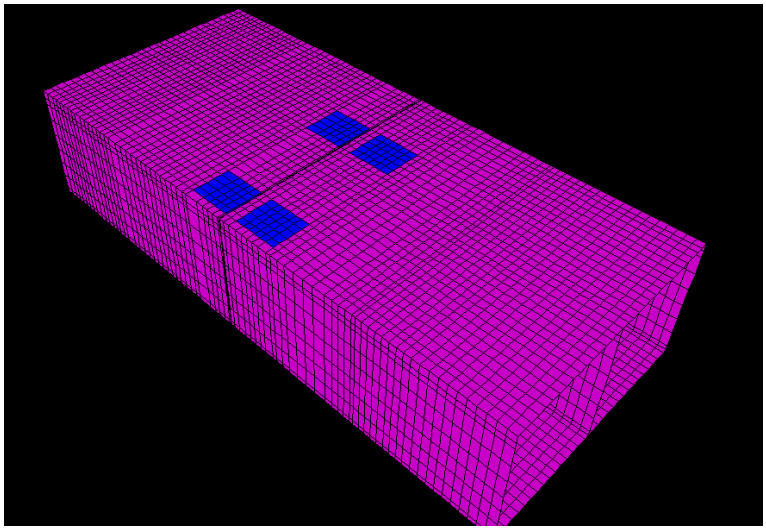

Figure 8
Separate wheel load distribution (Culvert #4)

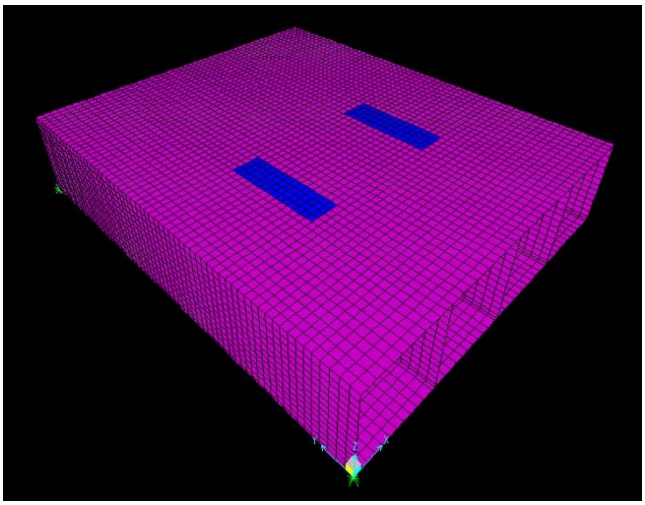

Figure 9
Overlapping wheel load distribution (Culvert #8)

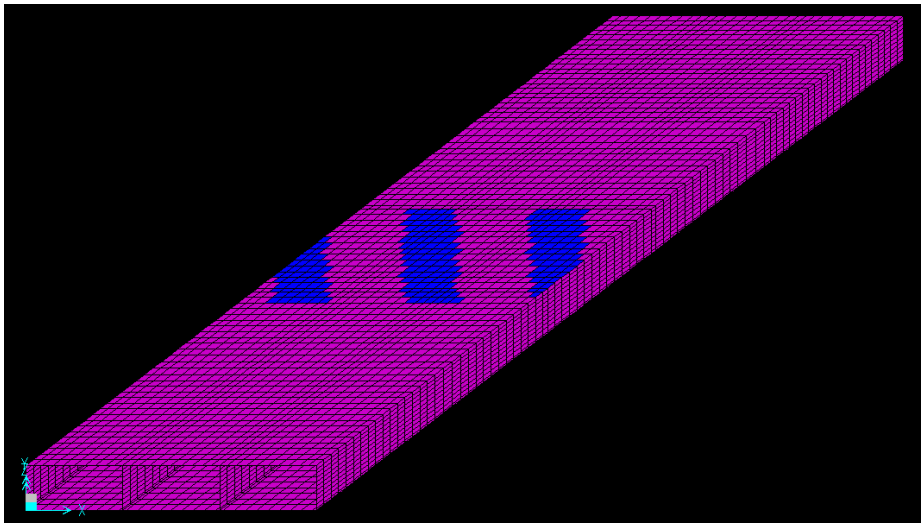

Figure 10
Wheel load distribution for a skewed culvert (Culvert #5)

Field Testing and Data Processing

Sensors are generally placed on and around the load path at critical locations to extract the maximum sensor readings corresponding to the peak structural response. This response represents the real structural behavior under loaded test truck, and hence, can be used to calibrate idealized FE models that may not account to factors that affect the structure's response; structural or nonstructural, due to inherent assumptions. To avoid unwanted signal noise, normal traffic was stopped with the help of DOTD district personnel shortly prior to the start of testing and was allowed to resume once the test truck completely passed over the culvert. Test trucks were positioned off the culvert at a distance equal to 20 ft. from the culvert's edge as a starting position. Once the research team signaled, the truck was driven on a straight load path around an idle speed (5 mph). The position of the truck was monitored by recording an automatic timestamp every one full tire revolution until the truck was cleared off the culvert. The tire circumference was measured from the average of 5 full tire revolutions. Therefore, the data obtained during load testing can be represented in time and truck position scales. Thus, the truck position versus the structural response were directly related, which was used for FE model calibration by positioning the model truck on any load path, and interpolating the structural response between the known truck positions. It should be noted that the data collection frequency was 50 Hz.

Finite Element Model Development

Three-dimensional (3D) Finite Element (FE) models were developed to rate the selected culverts. The use of 3D FE models was deemed necessary for obtaining realistic live load distributions, which cannot be captured by the commonly used 2D models. They can also

capture the effect of axle loads as they travel over the culvert in a more comprehensive way. The main inputs to build these models and to understand the structural behavior are the structural dimensions and material properties obtained from standard project details and field live load tests. The structural response from field testing of the culverts considered in this project were utilized as an input to calibrate the finite element models.

Despite the superiority of 3D FE modeling, it is not a practical approach for daily culvert rating because of the cost of time and computational resources required for building such models. Nevertheless, it can be used for specific cases that other methods are rendering unacceptable such as the case for all but one of the eight culverts considered in this study. There are several options for building 3D FE models. Initially, solid and shell elements were investigated to compare their advantages and disadvantages. It was concluded that using shell elements with their 6 degrees of freedom (DOFs) was more efficient than the solid elements. This is due to the fact that shell elements allow direct access to nodal solutions (moments, shear forces, etc.) at each node; whereas, solid elements have only 3 DOFs resulting in stresses that will have to be post-processed to obtain nodal forces in order to be able to perform load rating calculations. Furthermore, the number of nodes is higher for the same size model with solid elements; therefore, the total run time considering the calibration of the culvert and analysis of each design and legal trucks was reduced by using shell elements. Finally, the implementation of rotational springs at slab/wall connections would have become challenging if solid elements were to be used as constraint equations will be needed to relate rotations to solid element translation DOFs. Based on all of the above, it was concluded that shell elements will be used in this study.

One of the challenges associated with using shell elements is the need to represent offset connections which do not exist in real structures. Shell elements are typically positioned at midsection of the member they represent; e.g., wall or slab. At the juncture where the wall and the slab sections are connected, the slab's clear span length is increased by the sum of the half thicknesses of neighboring walls. The same is also true for the clear wall height in where the sum of the slab half thicknesses were added. Consequently, larger straining actions would result from a shell model that does not address this approximation resulting from idealized shell element models. Therefore, the connection detail was modified by assigning rigid elements at both ends of wall height and slab length equal to half the connected member thicknesses; i.e., slab and wall. The unmodified FE shell element connections are shown in Figure 11. In addition to the wall and slab offset, the tested culverts included a haunch at the top slab/wall connections. These haunches add to the rigidity of the connections, further reduce the slab and wall clear lengths. Therefore, it was also assumed that the rigid element section extended beyond the aforementioned half slab or half wall thickness by two-thirds of

the haunch length due to presence of additional concrete thickness. The rigid concrete area is shown in Figure 12 for top corner location only. The same is also true for bottom connections, albeit without a haunch.

Finally, rotational springs were defined at the nodes located at the connections between the shell elements and the rigid shell elements representing the junctures. The rotational spring stiffness can be assigned values ranging between released to fixed condition corresponding to no moment; i.e., hinged joint, or full continuity. Typical connection detail is given in Figure 13, and full scale culvert model can be seen in Figure 14.

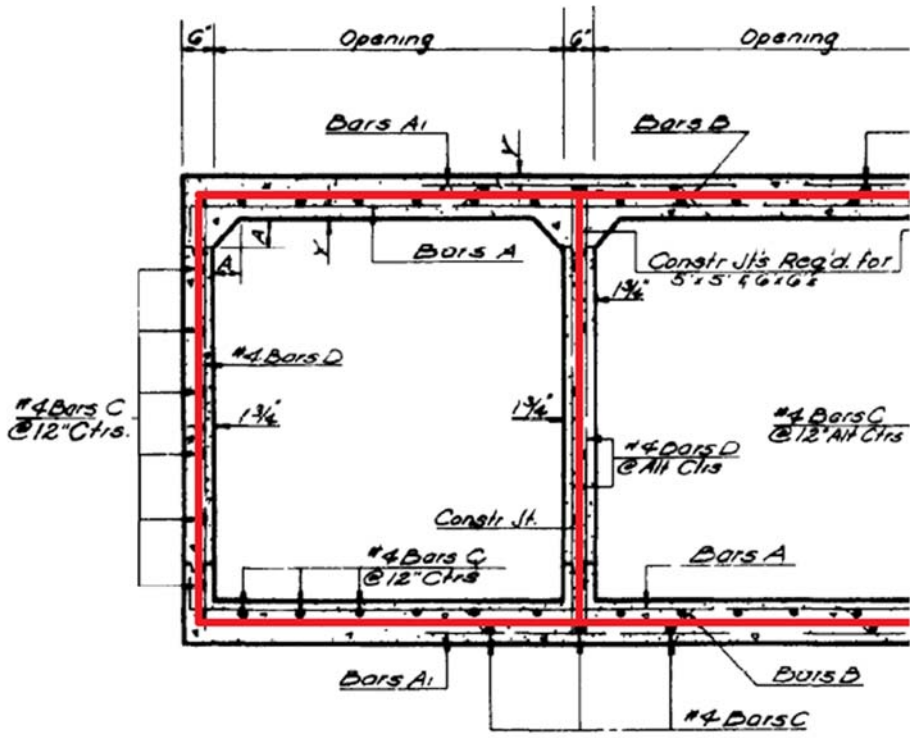

Figure 11
Unmodified shell element connections

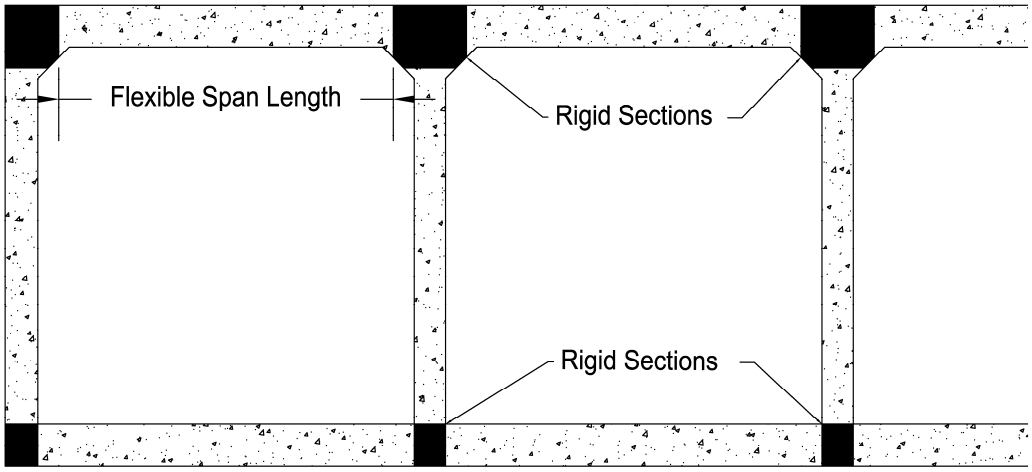

Figure 12
Rigid concrete region assumptions in FE model

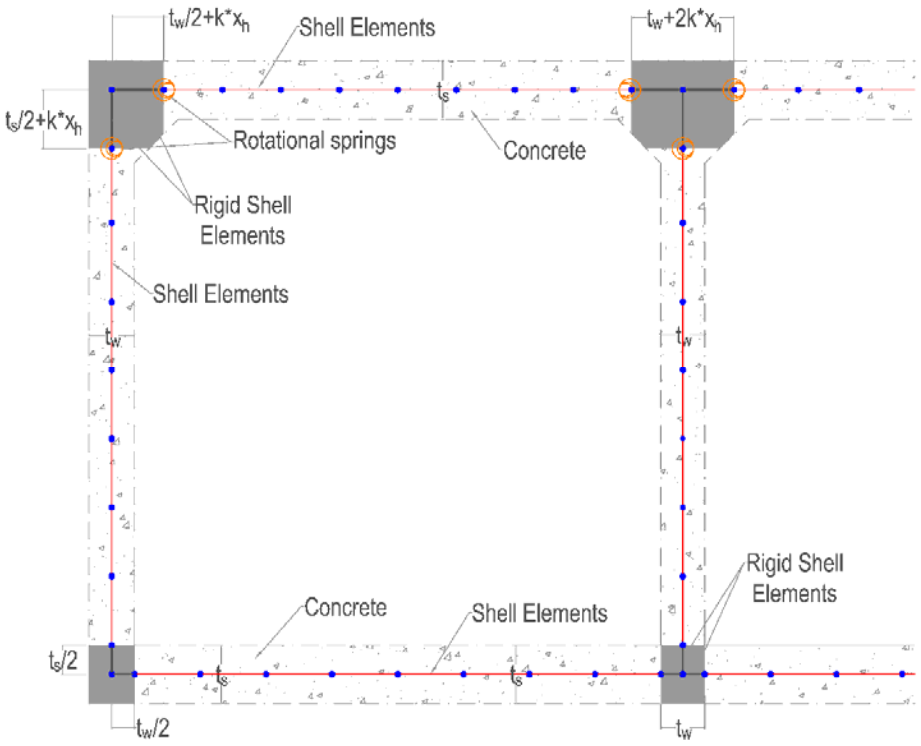

Figure 13
Typical wall- slab connection details in FE models

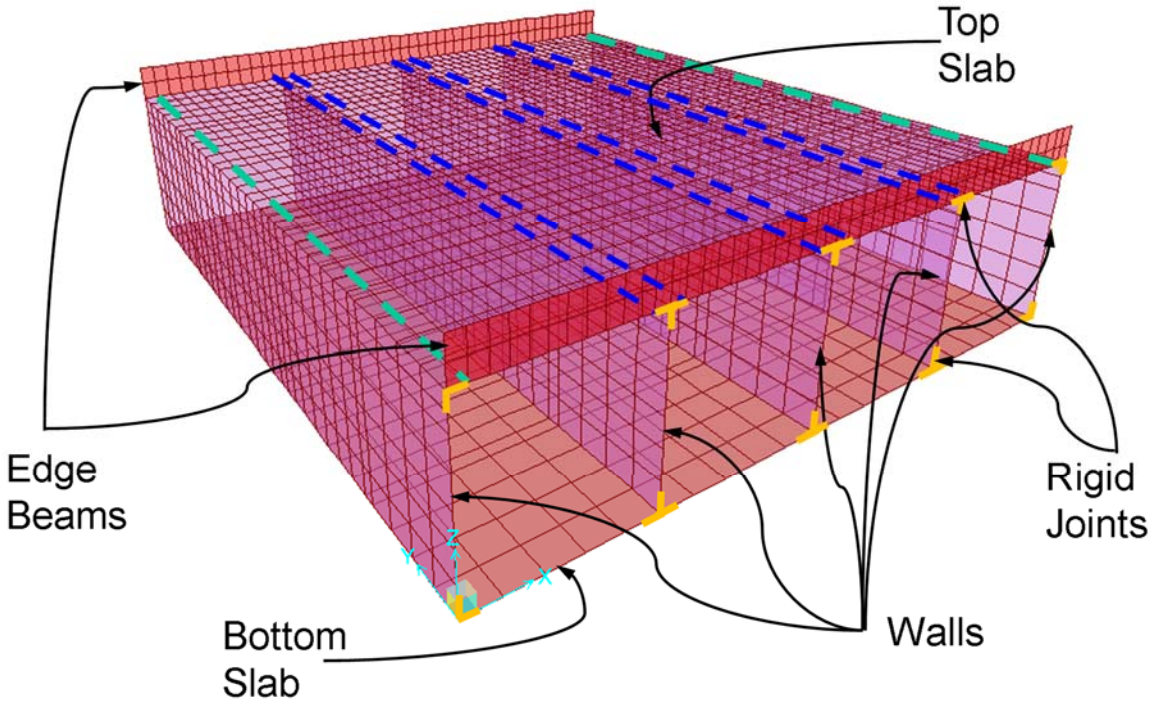

Figure 14
Full scale 3D FE model

Backfill-Structure Interaction

The exterior wall of the culverts typically retains soil materials. Lacking specific information about the soil type, compaction or placement, whether through testing or project documents, led the authors to make initial assumptions for the backfill soil-structure interaction model. The soil-structure interaction is modeled by introducing compression only springs perpendicular to the outer walls which are grounded to nodes. One section view of the backfill springs can be seen in Figure 15. The spring stiffness properties were calibrated using sensor data from the conducted field load tests by minimizing the rotational error. Since compacted backfill material properties could be assumed constant through in the depth of backfill and since the mesh size is closely distributed over the wall height and length, a single spring stiffness property was assigned to each node on the exterior wall. Two limit cases were studied for each culvert so that the spring model definition can be quantified in FE model definition; namely rigid non-linear soil springs (compression only) and released non-linear soil-springs (zero stiffness).

Assuming a compression-only rigid backfill in the FE model allows the exterior walls to deflect inwards. This means that no outward deflection is expected, therefore, the obtained

wall rotations were only a fraction of the experimentally recorded wall rotations. On the other the other hand, releasing the compression stiffness resulted in a maximum rotation equal to 0.0019°, which was closer to the experimentally obtained 0.0022° value. Another measure confirming this observation was that the maximum measured vertical strain in the wall was 11.1 $\mu\varepsilon$, compared to FE obtained values of 8.3 $\mu\varepsilon$ and 10.4 $\mu\varepsilon$ for rigid and released soil spring properties, respectively. Furthermore, the maximum vertical mid-span deflection was -0.0026 in. in the experimental readings. The same deflection was measured -0.0025 and -0.0028 in. for rigid and released soil spring properties, respectively. Therefore, it was concluded that the rotational springs a major influence on deciding whether to include the backfill stiffness in our final FE models. The effect of soil stiffness on the behavior of exterior wall rotation is presented in Figure 16.

It should be mentioned that it is acceptable to assume that the vertical and horizontal earth pressures, which create opposite rotations on exterior walls, acted on the tested culverts prior to conducting the live load testing. This initial condition is excluded in FE analysis results presented later since the sensors readings were zeroed before each load test to establish a new baseline from which live load effects are measured. The reason is that the nonlinear soil springs can be activated with respect to their at-rest, un-deformed, position only, i.e., not with respect to the deflected position due to preexisting loads. For example, assuming that the horizontal pressure is dominant and the exterior wall has deflected inward, no spring reaction should be activated until the wall deflects under live load in the opposite direction to the original location. Once a wall node passes the original location, the non-linear springs becomes under compression, which does not represent the real structural behavior based on the measured sensor data. Therefore, the calibration of the FE models with non-linear springs was studied assuming zero initial conditions. The results showed that a back-fill spring stiffness does not allow the exterior walls to rotate freely, and that removing the springs provides similar rotations to what was measure during field testing. Therefore, it was concluded the assigned backfill springs can be considered redundant based on the aforementioned findings. Therefore, they were excluded from final calibrated FE models.

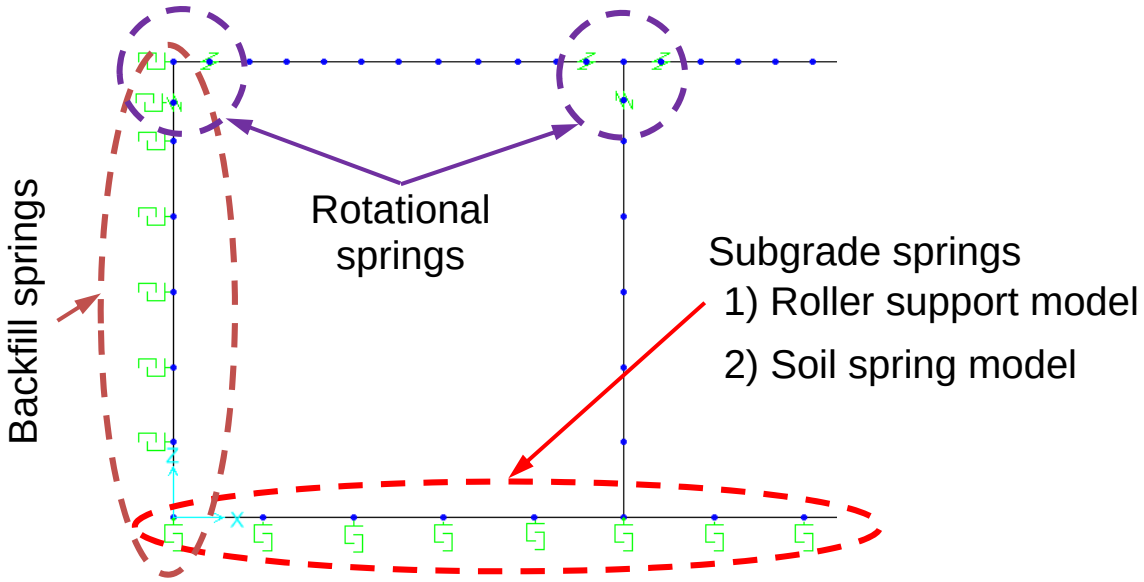

Figure 15
Exterior wall and bottom slab soil interactions using non-linear springs (compression only)

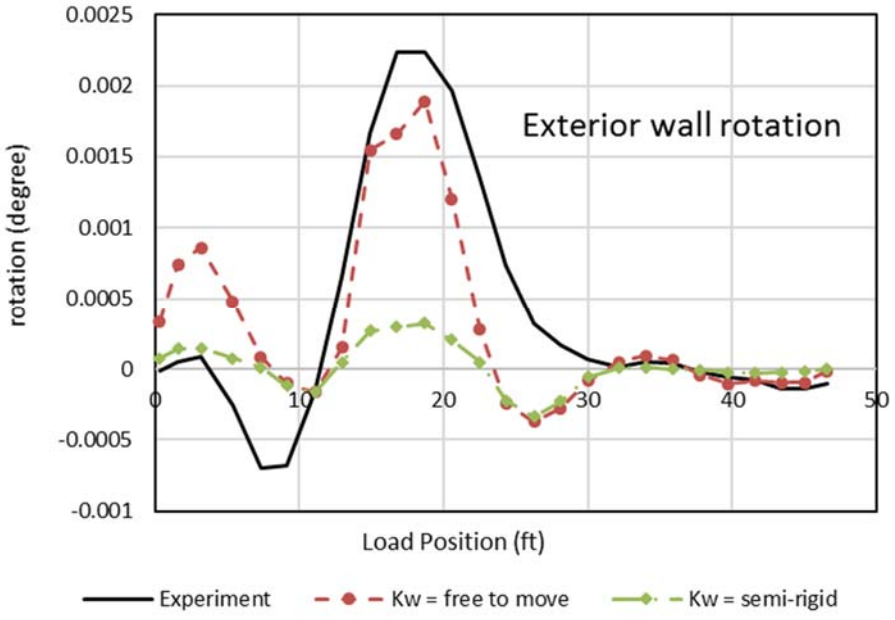

Figure 16
Exterior wall sensor location and rotation with stiffness = 0 and stiffness ≥ 0

Subgrade-Structure Interaction

A parametric study was conducted on one of the culverts to investigate the change of structural forces and deformations for various soil-structure interactions. All the structural properties except subgrade interaction were kept same in this study. All interior slab to wall

connections were assumed rigid, and exterior slab to wall connections were assumed to be hinged at the wall end. Nonlinear spring elements were assigned at each bottom slab node in the vertical direction to model subgrade soil-structure interaction behavior. The stiffness of all subgrade soil springs were calculated using two assumed subgrade modulus, k (pci). In addition to assuming springs to represent subgrade soil resistance, another model was developed where it was assumed that the bottom slab was supported on rollers at each bottom slab node. In all, three different cases were considered: 1) k = 150 pci, 2) k = 250 pci, and 3) k = roller support. Axial, moment and shear forces at maximum moment location, mid-span of culvert opening, were extracted from these models and are listed in Table 5. The design is mainly controlled by the moment forces; which according to the results in Table 5, its maximum variation was found to be about 4.0%. Table 6 lists the maximum deflected joint around the mid-span of the first culvert barrel excluding dead load effects. The experimental displacement at the same location then can be compared with the results obtained from the three considered FE models. The relative error between the three cases is important to understand the subgrade modeling effect on the structural response of the culvert, which is what impacts rating factors. The maximum variation in terms of maximum deflection for the top slab for the three different cases was 4.3%.

In addition to this limited parametric study, other studies TX DOT, reported that the subgrade has almost negligible effect to the rating factor *[21]*. Therefore, considering the amount of analysis time for FE model calibration and load rating analysis for minimal improvement in structural response quality, it was assumed roller supports (Case 3) for the bottom slabs would suffice for the goal of the project; i.e., culvert load rating. It was also noted that when the subgrade stiffness was assigned for one of the preliminary study culverts using Case 1 and 2 properties, the obtained rating factors were slightly higher for bending moments and slightly lower for shear forces. Therefore, it was concluded that if the rating factor is around 1.0, subgrade stiffness may have to be considered to obtain more accurate results. Otherwise, changing the subgrade stiffness will not greatly affect the rating factor.

Table 5
Structural Forces with different subgrade properties

Case	A (kip/in)	M (kip-in/in)	V (kip/in)
1) k = 150 pci	0.0075	3.1737	0.0367
2) k = 250 pci	0.0051	3.1402	0.0359
3) k = roller	0.0077	3.0504	0.0358

Table 6
Mid-span deflection with different subgrade properties

Case	Δ (in)
1) k = 150 pci	-0.003140
2) k = 250 pci	-0.003180
3) k = roller	-0.003276

Rotational Springs

As described earlier, rigid sections were introduced at the connections between the culvert's walls and slabs in FE model (see Figure 13) to account for the joint's concrete bulk and to avoid overestimating straining actions in some locations while underestimating it in others. The standard details for the tested culverts showed that the wall/slab connections at exterior openings were reinforced with a single layer of reinforcement on the compression side of the concrete section; i.e., the tension, or upper, side is not reinforced. These connections are therefore not able to resist negative moments that develop at outside wall/slab connections. The purpose of the rotational springs is to represent discontinuity of moments at that corner sections providing zero rotational spring stiffness. The idea here is similar to the hinge connection in frame elements.

The rotational springs were only assigned at the slab/rigid section even though the wall also has a single layer reinforcement. It was assumed that the first crack would develop at the slab section and as a result of losing the slab's flexural rigidity at the hinge location, the moment at that connection would be released. Therefore, no moments would be transferred to the wall, and hence the uncracked assumption for the wall justifying the lack of need to assume another hinge in the wall. Furthermore, including many hinges in the model may render the model unstable, which would require adding sway restraining elements or boundary conditions. In summary, the rotational stiffness was assumed to be zero at one of the connections only regarding both wall or slab sections. In this study, it was assumed to be in the slab, which creates the largest moments in the slab. In other words, the crack was assumed at the slab/rigid connections, while the wall/rigid connections were assumed uncracked and full continuity was provided at these locations in the FE models.

The tested culverts did not have a haunch at the bottom wall/ lab connections. Therefore, the rigid region was assumed to extend to only half the thickness of the wall and slab sections. The standard details also showed that a single layer reinforcement existed in the bottom slab of the culvert. However, rotational springs were not included for the bottom slab connection due to the way subgrade reaction is typically distributed (i.e., around the walls) as a result of the subgrade effect.

Finite Element Model Calibration

In this section, the major steps used for calibrating the developed 3D FE models are described. Also, the method used for quantifying the difference between predicted and measured culvert response is presented.

Model Calibration

After developing an initial model using the earlier assumptions, this nominal model was first run with the provided project dimensions and material properties. It was clear that the measured response indicated that the performance of the culverts was stiffer than the predicted performance using nominal properties. An error function was used to optimize sensor behavior and magnitude. It is the research team's experience after conducting extensive runs that the important factor for the calibration was the thickness of the slab sections, which was difficult to obtain for a buried structure during field investigation. Therefore, the slab thicknesses were allowed to be increased by up to 15% if the field data were smaller than the FE model results. This increase falls within the allowable construction tolerances for slabs. It should be noted that even if the slab thickness was increased to match field test measurements, the load capacity of the sections was conservatively calculated using project's nominal thickness. In general, the error in strains was more than in displacements and rotations. Therefore, increasing the slab thickness within the limits reduced the error. However, increasing the slab thickness by more than 15% resulted in FE model displacements below the field measured LVDT readings. Therefore, the minimum error was obtained by optimizing the slab thickness. This iterative procedure was repeated until the estimated error is minimized. Error estimates below 20% were considered acceptable for such complex three-dimensional buried structures with many unknown parameters. The final FE model will be referred to as *calibrated* FE model and the rating trucks passed the culverts to obtain forces in critical sections.

Error Estimation

To minimize the error in the structural response obtained from the 3D FE models compared to the actual measure response obtained from field testing, a consistent method for error estimation had to be first established. In lieu of considering all sensors used in the load testing, the error percentage in these models are calculated using a modified second norm of the relative error between FE and experimental field results. The preliminary runs showed that including all sensors in error estimation resulted in exaggerated errors. This is due to the fact that not all sensors recorded readings at high levels. Sensors away from a certain truck load path recorded low readings, hence a difference between the estimated and measured reading could easily reach 50%. Therefore, error estimation was focused on the sensors that

are directly subjected to the axle load and exceeding a certain threshold magnitude which was defined 10% of the peak reading. Also, if the sensor data obtained from field tests did not meet the expected behavior or magnitude, it was disregarded in error calculations attributing the erratic result to installation issues or system malfunctions. The error function used in this study is given in equation (4).

$$Error = \sum^{N_{lp}} \left[\left(\sum^{n_{lp,i}} \sqrt{\left[\frac{(y_{exp} - y_{FE})}{y_{exp}} \right]^2} \right) * \frac{1}{n_{lp,i}} \right] * \frac{1}{N_{lp}} \quad (4)$$

where,

y_{exp} = Sensor data obtained from field test
y_{FE} = Sensor data obtained from FE model
$n_{lp,i}$ = Number of sensors used in one load path
N_{lp} = Number of load tested truck path

Load Rating

The critical sections were identified for one exterior and one interior barrel. Nine different locations were considered for bending moment, shear forces and axial (thrust) forces as shown in Figure 17. The maximum and minimum forces were extracted from the straining action envelopes obtained using the calibrated 3D FE models. Appropriate load factors were assigned to each straining action following AASHTO provisions. The minimum load factor was applied when the load caused a reduction in the overall load effects at a certain critical section, and the maximum load factor was applied when the load caused an increase in the overall load effects. Dynamic load allowance, or impact factor, was included in calculations of rating factor, and reduced linearly when the fill height increased per AASHTO LRFD Design 3.6.2.2 *[4]*.

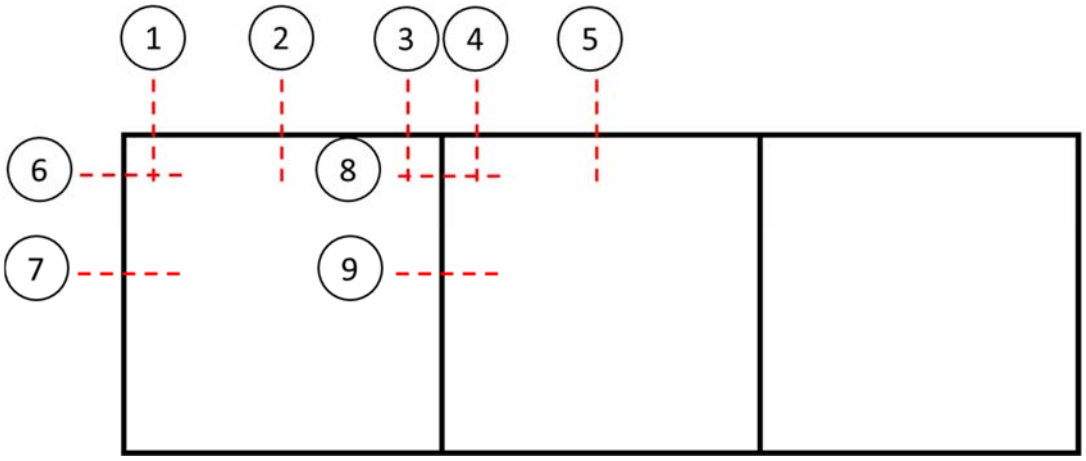

Figure 17
Critical sections for rating factor calculations

Moments at the mid-span of the barrels are typically subjected to positive moments only. Hence, Sections ② and ⑤ in Figure 17 were used obtain maximum bending moments noting that the maximum moment occurs at the exterior barrel. Negative moments were evaluated at section ③ and ④ in Figure 17. However, the negative moment was not considered due to existence of rotational springs at the exterior wall/slab connection where zero rotational stiffness were provided. Sections ①, ③, and ④ were used to obtain shear forces, and Sections ⑥, ⑦, ⑧, and ⑨ were used only to calculate thrust forces. Rating factors for thrust forces are calculated without considering the axial-flexural force interaction and only 10% of factored nominal capacity accounted for the rating factor unless it was less than 1.0. Rating factors were calculated for each critical section and the minimum rating factor from all sections was identified and the corresponding section was listed as an indicating of the controlling straining action (bending moment, shear force, and thrust).

In this study, the live load test trucks used in testing the culverts are three-axle dump trucks, and typically the rear axle distance was 6 ft. wide. The truck dimensions and axle loads were measured right before each test. Table 7 lists the truck details for each of the tested culverts. Because Culverts #7 and #8 were tested in two consecutive days and were in the same district, the same truck was used for testing both of them, hence the properties given in the table are identical for these two culverts.

Table 7
Test truck's GVW and axle spaces

Culvert #	Test Truck GVW (lb)	Front Axle (lb)	Rear Axles (total) (lb)	Front Axle Spacing (ft. – in.)	Rear Axle Spacing (ft. – in.)
1	48,253	11,004	37,249	12' – 2"	4' – 7"
2	57,134	12,604	44,530	12' – 0"	4' – 6"
3	57,265	12,890	44,375	12' – 0"	4' – 6"
4	51,581	12,995	38,586	13' – 1"	4' – 6"
5	52,100	12,350	39,750	12' – 0"	4' – 4"
6	53,619	11,415	42,204	12' – 3"	4' – 5"
7	42,150	9,540	32,610	12' – 0"	4' – 5"
8	42,150	9,540	32,610	12' – 0"	4' – 5"

One design truck, HL-93 and 10 legal trucks were considered for evaluating the selected culverts considered in this study. These trucks and their gross vehicle weight, GVW, are given in Table 4. The load ratings were completed for the design and all legal trucks even though rating legal truck is not required per AASHTO's *Manual for Bridge Evaluation* (MBE) specifications if the design truck's rating factor is larger than 1.0 *[20]*.

Nominal section capacities were calculated using AASHTO LRFD provisions *[4]*. The sectional properties and reinforcement details of the eight selected culverts are given in Table 8. It should be noted that the reinforcement's yield stress was assumed according to AASHTO's Manual for Bridge Evaluation (MBE) 6A.5.2.2 *[20]*. A constant modulus of elasticity for the steel reinforcement (E_s) equal to 29,000 ksi was used for all culverts. The flexural capacities are calculated per AASHTO LRFD Equation 5.7.3.2.2-1 and assuming the concrete cover is 1.75 in. for all the culverts. Similarly, the shear capacity was calculated per AASHTO LRFD 5.8.3.3 ignoring the existence of shear reinforcement, e.g., bent up bars in the slab at interior walls. Finally, the axial capacity was calculated using AASHTO LRFD 5.7.4.5 without considering axial-flexural interaction, respectively. It should be noted that the axial capacity is reduced 10% per AASHTO LRFD 5.7.4.5 to calculate the axial rating factors. The nominal member resistance of 8 culverts are given in Table 9.

Table 8
Section and reinforcement details of the culverts

Culvert #	Thickness (in).		Top Slab at Midspan				Top Slab at Connection with Interior Wall				f_c' (psi)	f_y (ksi)
	Slab	Wall	Top Reinforcement		Bottom Reinforcement		Top Reinforcement		Bottom Reinforcement			
			Size (#)	Spacing (in.)	Size (#)	Spacing (in.)	Size (#)	Spacing (in.)	Size (#)	Spacing (in.)		
1	8.5	7.0	-	-	6	7.0	6	7.0	6.0	14.0	6,326	40
2	8.0	6.0	-	-	6	7.0	6	7.0	6.0	14.0	6,693	40
3	9.0	8.0	-	-	6	6.0	6	6.0	6.0	12.0	8,948	40
4	12.0	12.0	-	-	7	6.0	7	6.0	7.0	12.0	8,971	40
5	8.5	7.0	-	-	6	6.5	6	6.5	6.0	13.0	10,662	40
6	7.5	6.0	-	-	5	5.0	5	5.0	5.0	10.0	9,018	40
7	8.0	6.0	-	-	6	6.0	6	6.0	6.0	12.0	9,268	40
8	9.0	8.0	-	-	6	6.0	6	6.0	6.0	12.0	7,158	33

Table 9
Nominal section capacities

Culvert	M_{cr} (kip-in /in.)	M_r (+) (kip-in /in.)	M_r (-) (kip-in /in.)	V_r (kip/in.)	A_r (kip/in.)
1	7.20	12.29	-13.47	0.97	37.00
2	6.50	11.38	-12.61	0.84	33.80
3	9.60	15.50	-16.98	1.24	59.80
4	17.00	29.90	-31.65	1.70	89.70
5	9.50	13.39	-14.85	1.32	65.27
6	6.70	10.24	-11.53	1.02	45.45
7	7.70	13.33	-14.81	1.10	46.40
8	8.50	15.40	-17.92	1.17	47.71

The equation used for calculating the rating factor given as

$$RF = \frac{C \pm \gamma_{DC} DC \pm \gamma_{DW} DW \pm \gamma_{EV} EV \pm \gamma_{EH} EH \pm \gamma_{ES} ES}{\gamma_{LL} * (LL + IM) \pm \gamma_{LL} * LS} \quad (5)$$

In which for the strenth limit states;

$C = \phi_c \phi_s \phi R_n$

where,

RF = Rating factor
C = Capacity
R_n = Nominal member resistance
DC = Dead load effect due to structural components
DW = Dead load effect due to wearing surface
EV = verical earth pressure
EH = horizontal earth pressure
ES = uniform earth surcharge
LL = live load effect
IM = dynamic load allowance
LS = live load surcharge
γ_{DC} = LRFD load factor for structural components
γ_{DW} = LRFD load factor for wearing surface
γ_{EV} = LRFD load factor for verical earth pressure
γ_{EH} = LRFD load factor for horizontal earth pressure
γ_{ES} = LRFD load factor for uniform earth surcharge
γ_{LL} = evaluation live load factor
γ_{LS} = LRFD load factor for live load surcharge
ϕ_c = condition factor
ϕ_s = system factor
ϕ = LRFD resistance factor

It should be noted that both the condition and system factors, ϕ_c and ϕ_s, were taken as 1.0, while the resistance factor was taken from AASHTO-LRFD Design Table 12.5.5-1.

RESULTS AND DISCUSSIONS

In this section, FE model calibration results are presented for Culvert #1 as a demonstration of the procedure adopted in this study. A summary of all the calculated rating factors for each culvert are also provided and the results are discussed.

FE Model Calibration of Culvert #1

Culvert #1 was the first culvert to be tested in this project and is used here to demonstrate the procedure for calibrating the developed 3D FE models. All preliminary models were developed following the major steps discussed earlier in "Finite Element Model Development".

The calibration process can be summarized by considering 4 main attempts as an example of the iterative procedure followed in this study. The properties used in the 3D FE model of Culvert #1 are given in Table 10. The analysis results presented later are for the second load path, which is near where all the tiltmeters were installed. The test trucks were driven on the other load paths, first and third, to obtain an overall average error for the culvert. As stated earlier, only sensors under the considered load path were used in calculating the estimated error. Case 1 is based on the nominal concrete properties and slab thickness given in standard drawings. The rotational stiffness in exterior slab wall connection was assumed zero due to lack of reinforcement capable of resisting negative moments in drawings. Despite that, the cross-sectional resistance at the exterior connections should not be taken equal to zero because even the one layer of reinforcement with a small effective depth can still resist a limited amount of negative moments; i.e., should not be taken equal to zero as is the case with currently used rating programs. Nevertheless, the negative moment resistance was neglected in our analyses due to the lack of applied moments at these connections as a result of the assumed rotational springs with zero stiffness.

The estimated error between Case 1 results and the experimentally obtained sensor readings using the error function given in Equation (4) was found to be 113%. In Case 2, the experimental concrete properties were used and the slab thickness was increased by 10% resulting in a reduction in the estimated error to 19.6%. Assuming the existence of exterior reinforcement, Case 3 provides 2.4% less error than Case 2, however this is technically not the case for the selected culvert group. Finally, in Case 4 the exterior rotational spring stiffness was kept at zero, and the slab thickness was increased 15%. The error in Case 4 was obtained 15.6%, which was the minimum of the compared cases. The behavior of sensors in different load positions are plotted in Figure 18 and Figure 19 for three sensors that were placed directly under the second load path. The difference in maximum strain data between

the nominal case and modified cases can be seen clearly in Figure 18, and the modified cases can be seen in Figure 19, which shows relatively smaller peak reading difference between the predicted and measured values. The difference in strain readings becomes smaller when 10% or %15 slab thickness is used in the 3D FE model. In addition to the strain sensor behavior, the nominal properties; i.e., Case 1, result in larger deflections that the other cases as shown in Figure 20. The displacement readings in Figure 21 for the same modified cases also decreases more when the 15% slab thickness is used; however, the error increases in the opposite direction and so does its contribution to the absolute total estimated error. Therefore, increasing the slab thickness further will not help reduce the estimated error. The slight differences in tiltmeter readings for the different analyzed cases can be seen Figure 22. One can see in Figure 23 that the exterior wall sensor, T1040, is in good agreement with the experimental rotations. This behavior confirms that the backfill stiffness can be neglected in the 3D FE model when live loads are applied.

Figure 24 and Figure 25 show the exterior barrel's corner strain data, and the interior barrel's corner strain data are shown in Figure 26 and Figure 27. The error in these plots is relatively much larger than the mid-span strain sensors shown in Figure 19. The error from these sensors whose readings are relatively low (e.g. < 10 $\mu\varepsilon$) unnecessarily increase the overall estimated error. Therefore, sensor readings with smaller magnitudes were excluded in error calculations.

Table 10
Culvert #1 FE model calibration case studies

Properties	**Nominal Properties**	**Modified Properties**		
	Case 1	**Case 2**	**Case 3**	**Case 4**
E_c (ksi)	3000	4573	4573	4573
t_{slab} (in.)	8.50	9.35	9.35	9.80
$K_{\theta,int}$ (kip/θ/in.)	Fixed	Fixed	Fixed	Fixed
$K_{\theta,ext}$ (kip/θ/in.)	0	0	Fixed	0
$Error$ (%)	113.0	19.6	17.2	15.6

E_c = Elastic modulus of concrete, t_{slab} = Slab thickness, $K_{\theta,int}$, $K_{\theta,ext}$ = Internal and external rotational spring stiffness

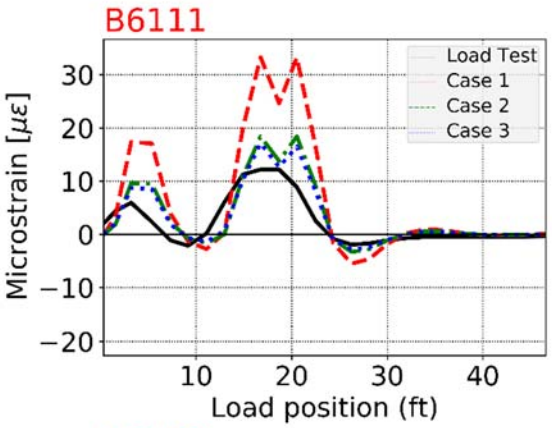

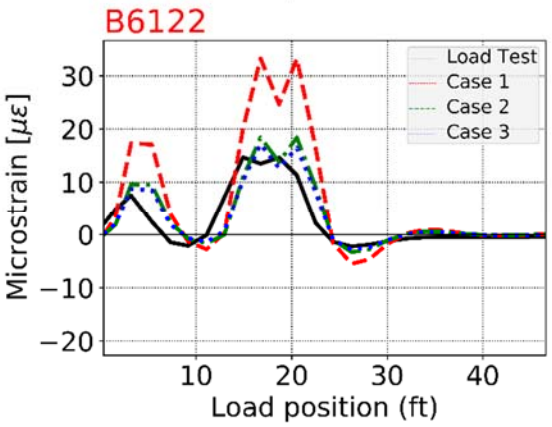

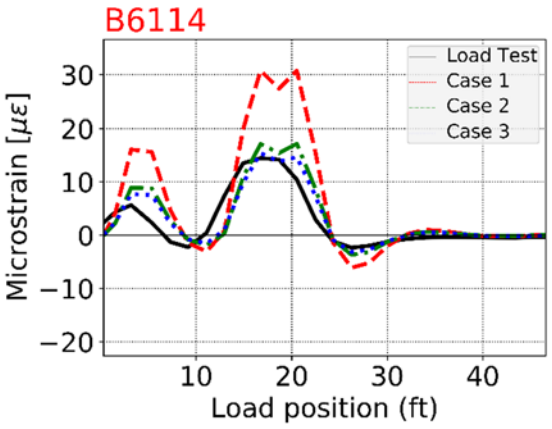

Figure 18
Mid-span strain data for nominal case (Case 1) and modified cases (Case 2 and 3)

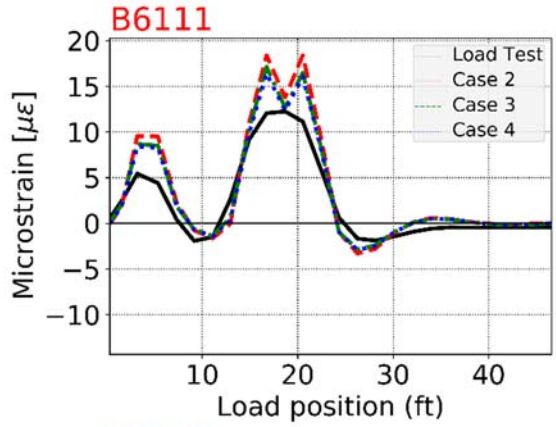

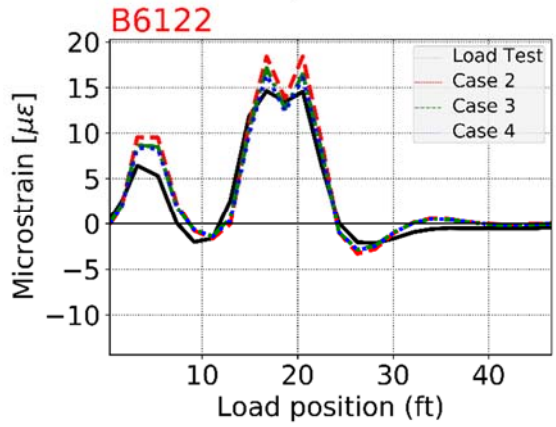

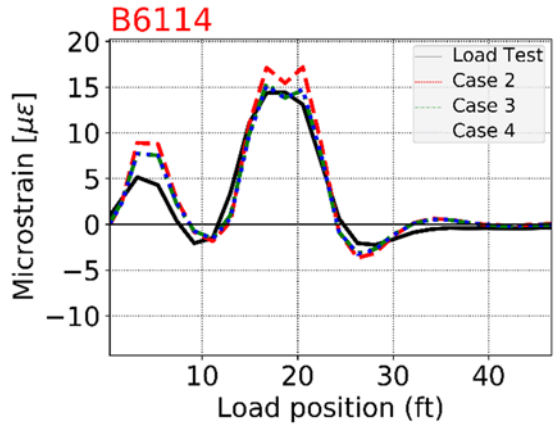

Figure 19
Mid-span strain data for modified cases (Case 2, 3, and 4)

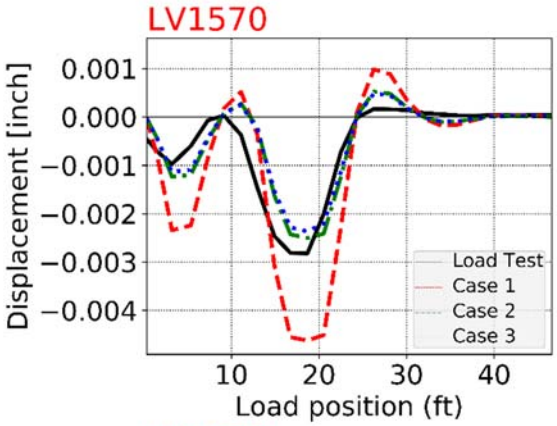

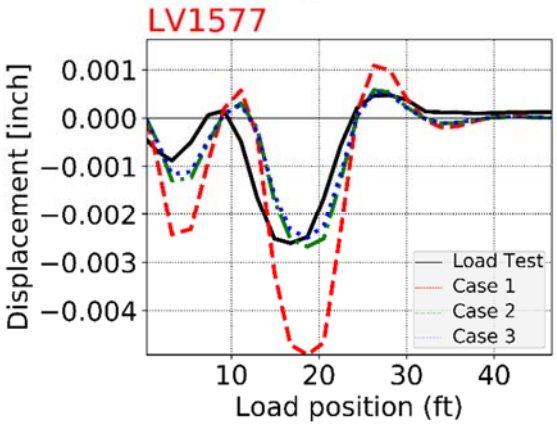

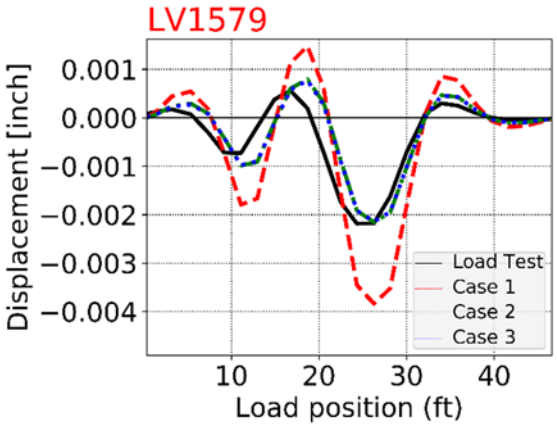

Figure 20
LVDT data for nominal case (Case 1) and modified cases (Case 2 and 3)

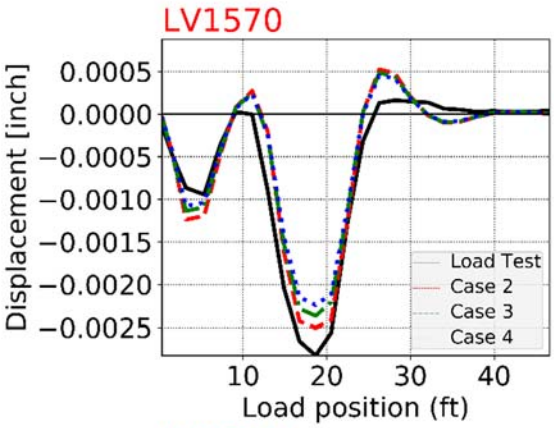

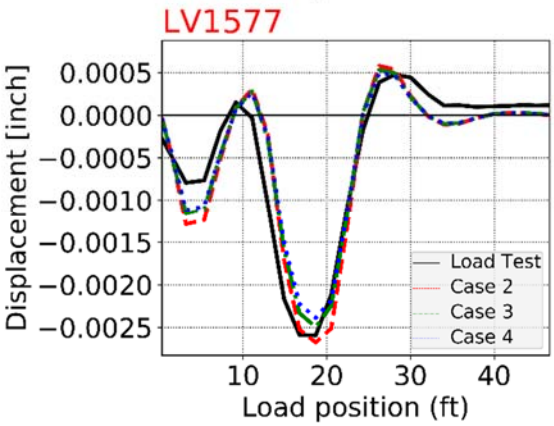

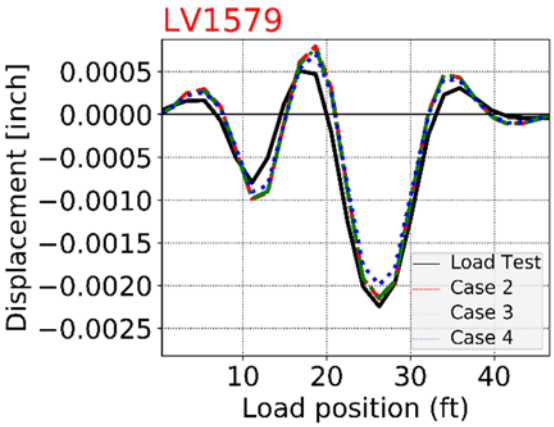

Figure 21
Mid-span strain data for modified cases (Case 2, 3, and 4)

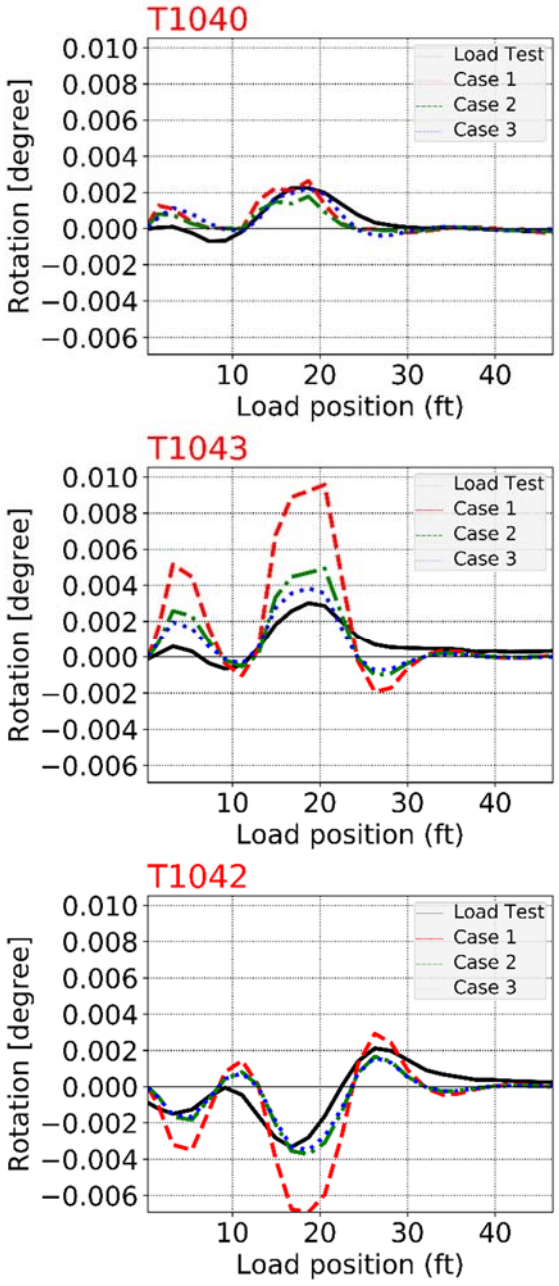

Figure 22
Tilt-meter data for nominal case (Case 1) and modified cases (Case 2 and 3)

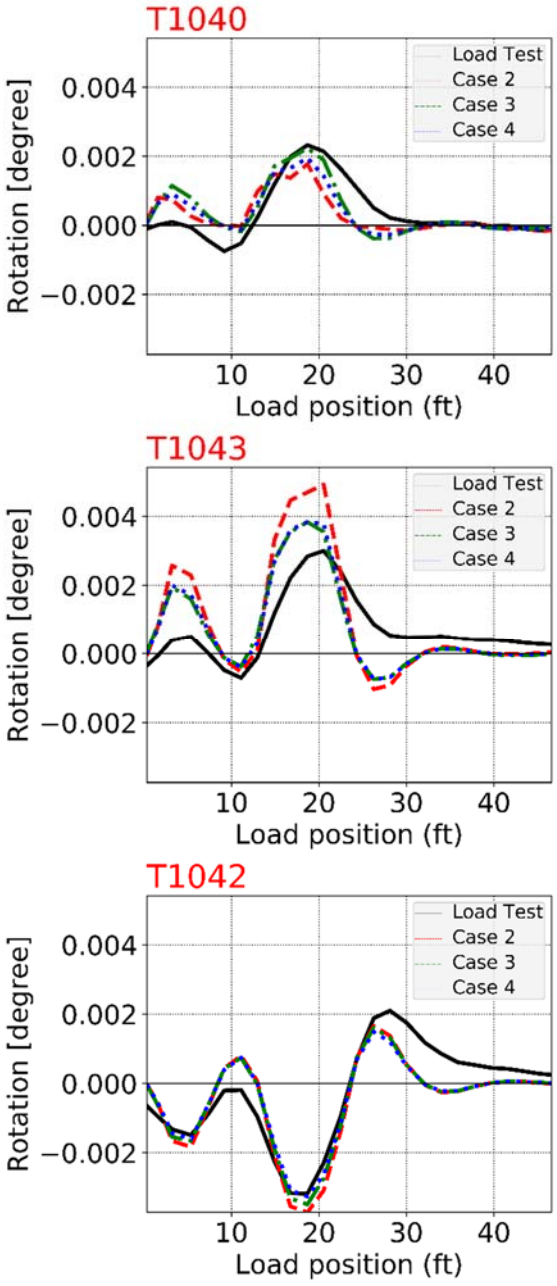

Figure 23
Tilt-meter data for modified cases (Case 2, 3, and 4)

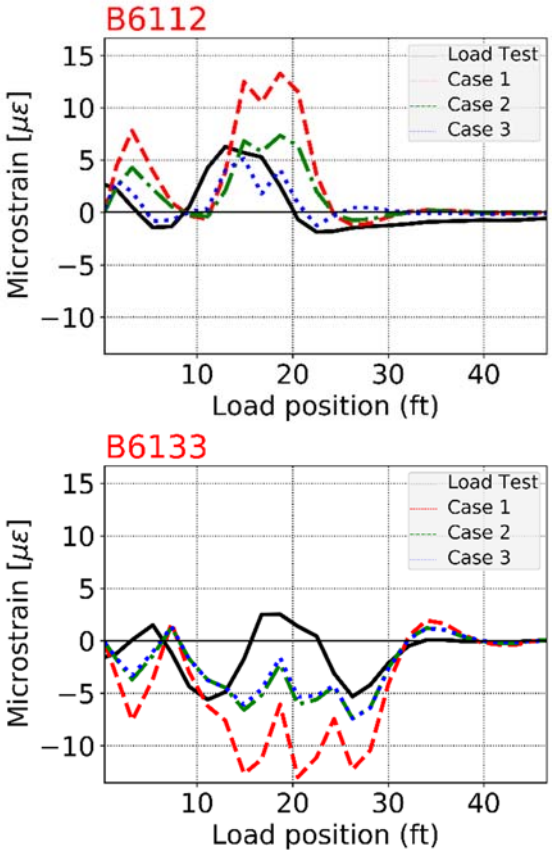

Figure 24
Exterior opening corner strain data for nominal case (Case 1) and modified cases (Case 2 and 3)

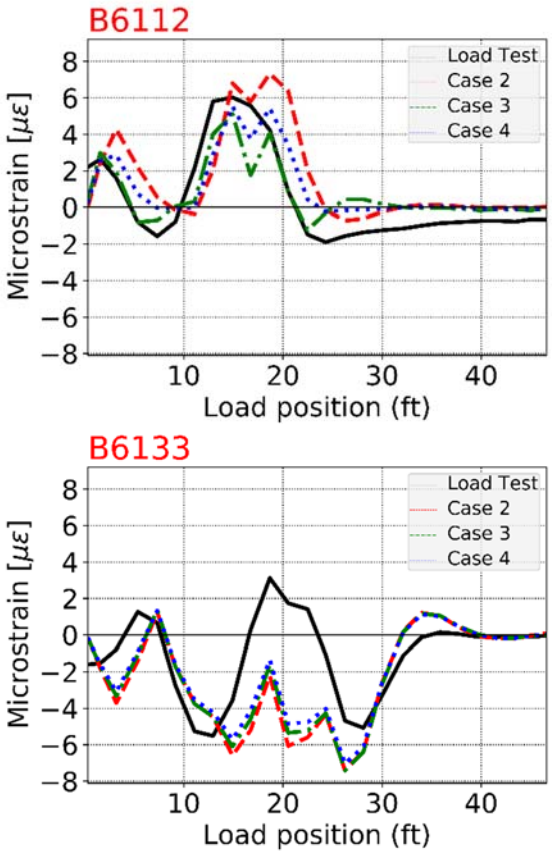

Figure 25
Exterior opening corner strain data for modified cases (Case 2, 3, and 4)

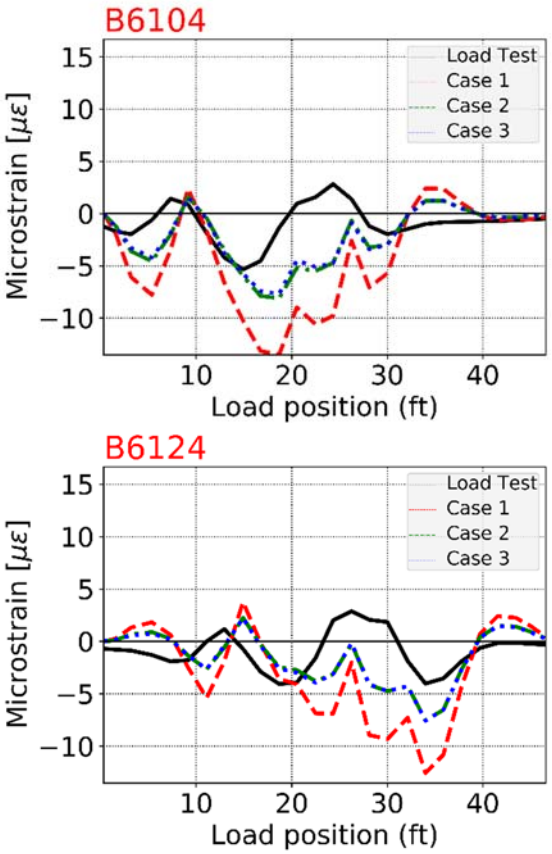

Figure 26
Interior opening corner strain data for nominal case (Case 1) and modified cases (Case 2 and 3)

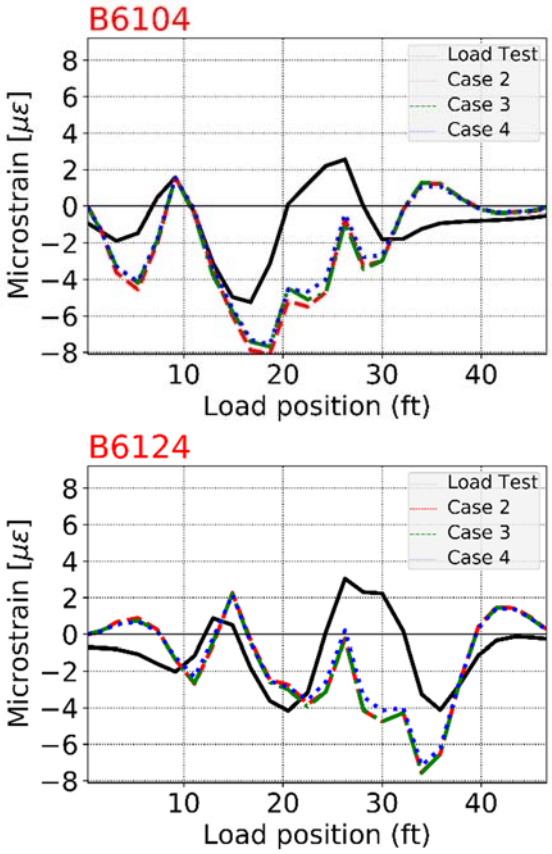

Figure 27
Interior opening corner strain data for modified cases (Case 2, 3, and 4)

Rating Results

In the calibration process, all three load paths were used to obtain an overall error percentage. However, the rating factor was obtained using only one path that produced the highest possible section forces. The second path was chosen because it is typically the path for long enough culverts such that the culvert's edges, and therefore the headwall interference with the axle load distribution is negligible. It is also typically the path that does not cross over an expansion joints. The summary of the rating factors and critical locations are given for each culvert in Table 11 through Table 18. It can be concluded from the FE analysis that the most critical section that controls the load rating typically falls in exterior opening top slab. The design truck, HL-93, at the inventory level produces the least rating factor for all the considered culverts, however, none of the culverts ratings dropped below 1.0 with a minimum inventory rating factor of 1.12 for Culvert #3, which has the least average fill height, 1.08 ft., and 8 ft. x 8 ft. clear cell openings that is the second widest opening between the representative eight culverts. The second smallest rating factor, 1.39, is obtained in

Culvert #4 which has 2.24 ft. average fill height with 12 x 12 ft. cell openings. At the operating level, three of the culverts' rating factors were calculated between 1.4 and 2.0, while the others had higher rating factors. Finally, the lowest rating factor for legal trucks was found to be 1.60.

In the exterior opening and mid-span moment or corner shear forces produce the least rating factor. It can be noted that even when the shear forces control the rating factor, the rating factor for the mid-span moment is also close to controlling rating factor. In other words, the rating factor for the mid-span section is either controlling the rating factor or slightly above the controlling factor. Recalling the FE model subgrade studies presented earlier with 150 pci subgrade stiffness, it was concluded that the roller (i.e., rigid) support reduces the moment forces by roughly 4% and the shear forces by roughly 2.4% when compared to the flexible subgrade. Since the subgrade under culverts is not actually rigid, the presented rating factors would be slightly less than the if the actual subgrade stiffness is considered. In a preliminary study of Culvert #1, it was revealed that the rating factors increased around 4% for controlling bending moment sections and reduced around 1% for shear force sections if a roller (rigid) support is assumed. Therefore, it is expected that some controlling critical sections will change from mid-span bending moments shear force controlling sections. Nevertheless, the change in rating factors for Culvert #1 to Culvert #8 become negligible for the culverts that has rating factor larger than 1.05.

Furthermore, it is worth noting is that the summation of the unfactored section forces at each critical bending moment sections poses less demand than the uncracked section capacities, i.e., cracking moment, M_{cr}, that is given in Table 9. This implies that the considered culverts may still be behaving as uncracked RC sections under service loads.

Another interesting result here is the relation between the fill height and span length. The change in rating factor with the ratio of fill height to span length is shown in Figure 28 for HL-93 inventory, HL-93 operational, LA Type 6 and Type 3-3 vehicles. The results shown in Figure 28 indicate that smaller fill height to span length ratios may possibly produce lower rating factor. This observation needs to be verified using a larger number of cases in a parametric study that looks into the effect of this ratio and other factors. A comprehensive study can also serve as the basis for producing more accurate axle load distribution equations that can be used in rating buried culverts.

Table 11
Culvert #1 Minimum load rating factors and critical sections

Vehicle Type	GVW (kips)	Rating Factor	Section Number	Section Location
HL-93 (INV)	N/A	1.98	3	Exterior Top Slab Corner Shear
HL-93 (OPR)	N/A	2.57	3	Exterior Top Slab Corner Shear
LA Type 3	41.0	3.85	3	Exterior Top Slab Corner Shear
LA Type 3S2	73.0	3.74	3	Exterior Top Slab Corner Shear
Type 3-3	80.0	3.19	3	Exterior Top Slab Corner Shear
LA Type 6	80.0	3.27	3	Exterior Top Slab Corner Shear
LA Type 8	88.0	4.21	3	Exterior Top Slab Corner Shear
NRL	80.0	3.61	3	Exterior Top Slab Corner Shear
SU4	54.0	3.67	3	Exterior Top Slab Corner Shear
SU5	62.0	3.66	3	Exterior Top Slab Corner Shear
SU6	69.5	3.66	3	Exterior Top Slab Corner Shear
SU7	77.5	3.66	3	Exterior Top Slab Corner Shear
Average Fill Height = 2.20 ft.; Wearing Surface = Asphalt				

Table 12
Culvert #2 Minimum load rating factors and critical sections

Vehicle Type	GVW (kips)	Rating Factor	Section Number	Section Location
HL-93 (INV)	N/A	4.57	3	Exterior Top Slab Corner Shear
HL-93 (OPR)	N/A	5.93	3	Exterior Top Slab Corner Shear
LA Type 3	41.0	10.68	3	Exterior Top Slab Corner Shear
LA Type 3S2	73.0	9.40	3	Exterior Top Slab Corner Shear
Type 3-3	80.0	7.42	3	Exterior Top Slab Corner Shear
LA Type 6	80.0	7.44	3	Exterior Top Slab Corner Shear
LA Type 8	88.0	9.69	2	Exterior Top Slab Center Moment
NRL	80.0	10.19	3	Exterior Top Slab Corner Shear
SU4	54.0	8.45	2	Exterior Top Slab Center Moment
SU5	62.0	8.44	2	Exterior Top Slab Center Moment
SU6	69.5	8.57	2	Exterior Top Slab Center Moment
SU7	77.5	9.29	2	Exterior Top Slab Center Moment
Average Fill Height = 7.00; Wearing Surface = Asphalt				

Table 13
Culvert #3 Minimum load rating factors and critical sections

Vehicle Type	GVW (kips)	Rating Factor	Section Number	Section Location
HL-93 (INV)	N/A	1.12	1	Exterior Top Slab Corner Shear
HL-93 (OPR)	N/A	1.40	1	Exterior Top Slab Corner Shear
LA Type 3	41.0	1.96	1	Exterior Top Slab Corner Shear
LA Type 3S2	73.0	1.87	1	Exterior Top Slab Corner Shear
Type 3-3	80.0	1.76	1	Exterior Top Slab Corner Shear
LA Type 6	80.0	1.60	1	Exterior Top Slab Corner Shear
LA Type 8	88.0	2.00	1	Exterior Top Slab Corner Shear
NRL	80.0	1.94	1	Exterior Top Slab Corner Shear
SU4	54.0	1.88	1	Exterior Top Slab Corner Shear
SU5	62.0	1.88	1	Exterior Top Slab Corner Shear
SU6	69.5	1.93	1	Exterior Top Slab Corner Shear
SU7	77.5	1.94	1	Exterior Top Slab Corner Shear
Average Fill Height = 1.08; Wearing Surface = Asphalt				

Table 14
Culvert #4 Minimum load rating factors and critical sections

Vehicle Type	GVW (kips)	Rating Factor	Section Number	Section Location
HL-93 (INV)	N/A	1.39	3	Exterior Top Slab Corner Shear
HL-93 (OPR)	N/A	1.81	3	Exterior Top Slab Corner Shear
LA Type 3	41.0	2.53	3	Exterior Top Slab Corner Shear
LA Type 3S2	73.0	2.27	3	Exterior Top Slab Corner Shear
Type 3-3	80.0	2.15	3	Exterior Top Slab Corner Shear
LA Type 6	80.0	2.16	3	Exterior Top Slab Corner Shear
LA Type 8	88.0	2.90	3	Exterior Top Slab Corner Shear
NRL	80.0	2.14	3	Exterior Top Slab Corner Shear
SU4	54.0	2.19	3	Exterior Top Slab Corner Shear
SU5	62.0	2.29	3	Exterior Top Slab Corner Shear
SU6	69.5	2.19	3	Exterior Top Slab Corner Shear
SU7	77.5	2.19	3	Exterior Top Slab Corner Shear
Average Fill Height = 2.24; Wearing Surface = Asphalt				

Table 15
Culvert #5 Minimum load rating factors and critical sections

Vehicle Type	GVW (kips)	Rating Factor	Section Number	Section Location
HL-93 (INV)	N/A	2.15	3	Exterior Top Slab Corner Shear
HL-93 (OPR)	N/A	2.79	3	Exterior Top Slab Corner Shear
LA Type 3	41.0	6.56	2	Exterior Top Slab Center Moment
LA Type 3S2	73.0	6.38	3	Exterior Top Slab Corner Shear
Type 3-3	80.0	5.69	2	Exterior Top Slab Center Moment
LA Type 6	80.0	5.73	2	Exterior Top Slab Center Moment
LA Type 8	88.0	7.42	2	Exterior Top Slab Center Moment
NRL	80.0	6.86	3	Exterior Top Slab Corner Shear
SU4	54.0	6.48	3	Exterior Top Slab Corner Shear
SU5	62.0	6.87	3	Exterior Top Slab Corner Shear
SU6	69.5	6.96	3	Exterior Top Slab Corner Shear
SU7	77.5	7.07	3	Exterior Top Slab Corner Shear
Average Fill Height = 4.14; Wearing Surface = Concrete				

Table 16
Culvert #6 Minimum load rating factors and critical sections

Vehicle Type	GVW (kips)	Rating Factor	Section Number	Section Location
HL-93 (INV)	N/A	2.57	3	Exterior Top Slab Corner Shear
HL-93 (OPR)	N/A	3.29	3	Exterior Top Slab Corner Shear
LA Type 3	41.0	4.79	3	Exterior Top Slab Corner Shear
LA Type 3S2	73.0	4.69	3	Exterior Top Slab Corner Shear
Type 3-3	80.0	4.12	3	Exterior Top Slab Corner Shear
LA Type 6	80.0	4.16	3	Exterior Top Slab Corner Shear
LA Type 8	88.0	5.25	3	Exterior Top Slab Corner Shear
NRL	80.0	4.25	3	Exterior Top Slab Corner Shear
SU4	54.0	4.31	3	Exterior Top Slab Corner Shear
SU5	62.0	4.35	3	Exterior Top Slab Corner Shear
SU6	69.5	4.25	3	Exterior Top Slab Corner Shear
SU7	77.5	4.25	3	Exterior Top Slab Corner Shear
Average Fill Height = 1.78; Wearing Surface = Asphalt				

Table 17
Culvert #7 Minimum load rating factors and critical sections

Vehicle Type	GVW (kips)	Rating Factor	Section Number	Section Location
HL-93 (INV)	N/A	1.61	2	Exterior Topslab Midspan Moment
HL-93 (OPR)	N/A	2.07	2	Exterior Topslab Midspan Moment
LA Type 3	41.0	3.40	2	Exterior Topslab Midspan Moment
LA Type 3S2	73.0	3.04	3	Exterior Top Slab Corner Shear
Type 3-3	80.0	2.63	3	Exterior Top Slab Corner Shear
LA Type 6	80.0	2.55	3	Exterior Top Slab Corner Shear
LA Type 8	88.0	3.47	3	Exterior Top Slab Corner Shear
NRL	80.0	3.28	3	Exterior Top Slab Corner Shear
SU4	54.0	2.74	3	Exterior Top Slab Corner Shear
SU5	62.0	3.21	2	Exterior Topslab Midspan Moment
SU6	69.5	3.15	3	Exterior Top Slab Corner Shear
SU7	77.5	3.24	3	Exterior Top Slab Corner Shear
Average Fill Height = 1.08; Wearing Surface = Concrete				

Table 18
Culvert #8 Minimum load rating factors and critical sections

Vehicle Type	GVW (kips)	Rating Factor	Section Number	Section Location
HL-93 (INV)	N/A	1.36	2	Exterior Top Slab Center Moment
HL-93 (OPR)	N/A	1.76	2	Exterior Top Slab Center Moment
LA Type 3	41.0	3.06	2	Exterior Top Slab Center Moment
LA Type 3S2	73.0	2.81	2	Exterior Top Slab Center Moment
Type 3-3	80.0	2.44	2	Exterior Top Slab Center Moment
LA Type 6	80.0	2.42	2	Exterior Top Slab Center Moment
LA Type 8	88.0	3.04	2	Exterior Top Slab Center Moment
NRL	80.0	2.99	2	Exterior Top Slab Center Moment
SU4	54.0	2.85	2	Exterior Top Slab Center Moment
SU5	62.0	2.85	2	Exterior Top Slab Center Moment
SU6	69.5	2.87	2	Exterior Top Slab Center Moment
SU7	77.5	2.98	2	Exterior Top Slab Center Moment
Average Fill Height = 1.60; Wearing Surface = Asphalt				

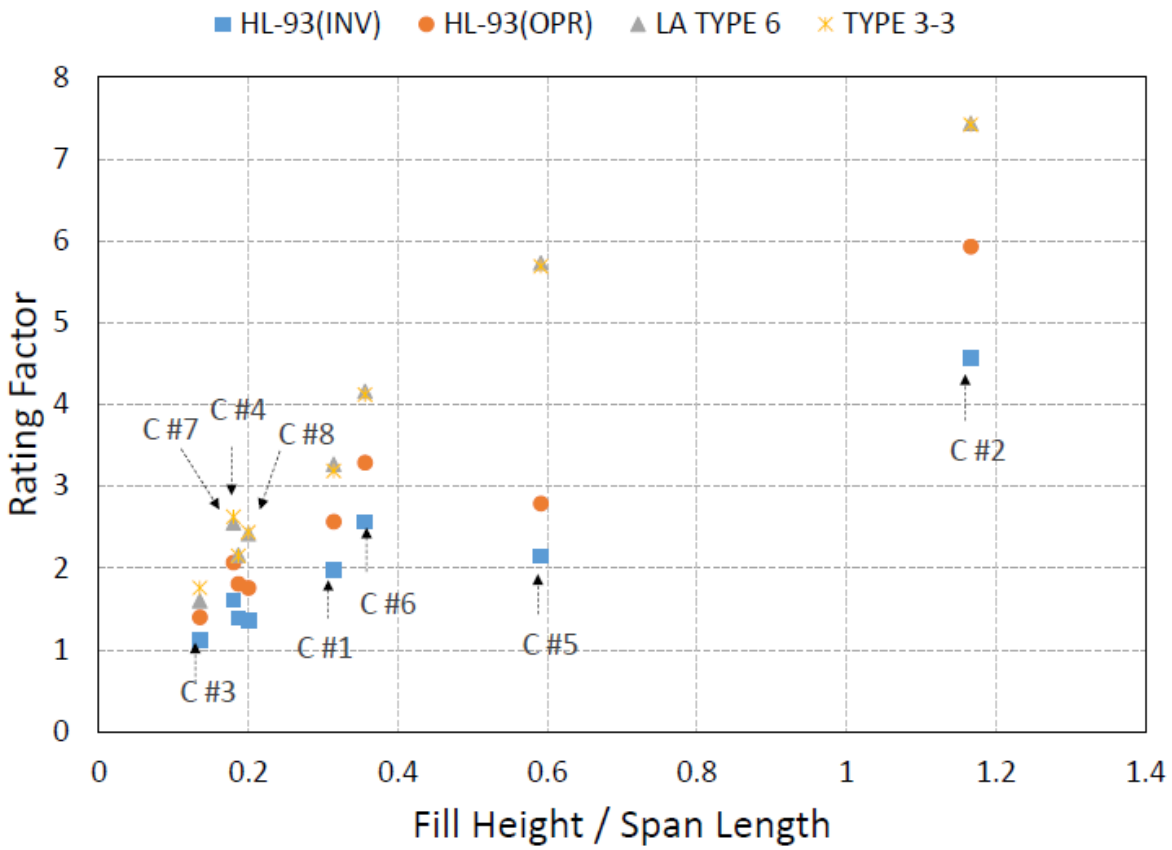

Figure 28
Rating factor for different fill height/span length ratios

Conventional Load Rating Results

Appendix D provides the load rating factors obtained for the selected culverts using traditional methods. It is clear that the rating factors are much lower than what the 3D FE models produced. The main reasons for the difference is that the conventional approach is not capable of capturing the true distribution of axel wheel loads on buried culverts.

Addressing 2D Modeling Challenges

Incorporating all the features described in this report in 2-D models is possible if the used software has such capabilities. However, not all software commonly used for rating bridge structures are flexible enough to allow for taking advantage of these structural attributes (rigid connections, intermediate hinges at locations other than the intersection of the members, etc.). In this section, a simple adjustment to input loads is presented for use in a software that is not capable of modeling rigid connections between culvert's slab and exterior wall.

The concept is based on a comparison of the resulting moments generated assuming the hinges are at a critical distance from the corner joint and assuming that they are exactly at the corner joint; i.e., with a shorter member length. This is illustrated in Figure 29. For a generic linear pressure distribution (p_1 and p_2) on an exterior wall, the length of the structural member representing the wall would differ depending on where the intermediate hinges are assumed. If the hinge is conservatively assumed at the intersection point between the slab and the wall, the member's length is, L, while it is only, L', if the hinges are assumed at the end of the rigid connections. In the latter case, the horizontal pressures at the beginning and end of the shorter member are p_1' and p_2'. The resulting bending moments at mid-height of the wall from both idealizations are M_{mid} and M'_{mid}, respectively. These moments can be easily calculated from equilibrium, resulting in

$$M_{mid} = \frac{p_1 L^2}{8} + \frac{(p_2 - p_1)L^2}{16} \tag{6}$$

and

$$M'_{mid} = \frac{p_1' L'^2}{8} + \frac{(p_2' - p_1')L'^2}{16} \tag{7}$$

where,

L = idealized member length assuming intermediate hinges at the wall-slab intersection
L' = idealized member length assuming intermediate hinges at the edge of rigid connections
p_1 and p_2 = horizontal pressure at the wall-slab intersection
p_1' and p_2' = horizontal pressure at the edge of the rigid connection
x_{cr1} and x_{cr2} = length of rigid connection along exterior wall

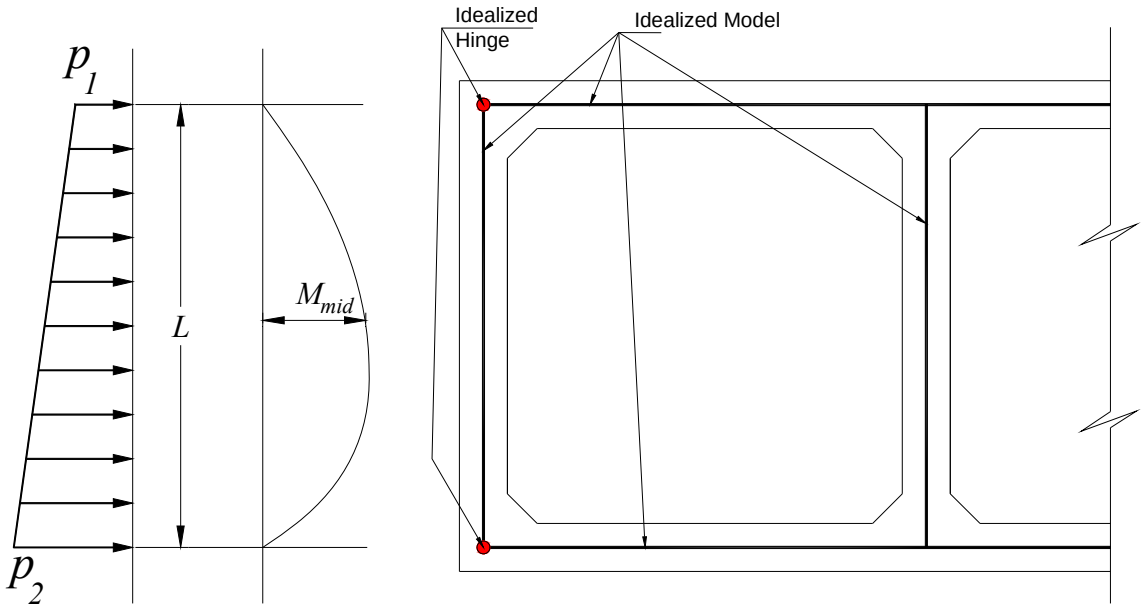

(a) Intermediate hinge at point of intersection between slab and wall

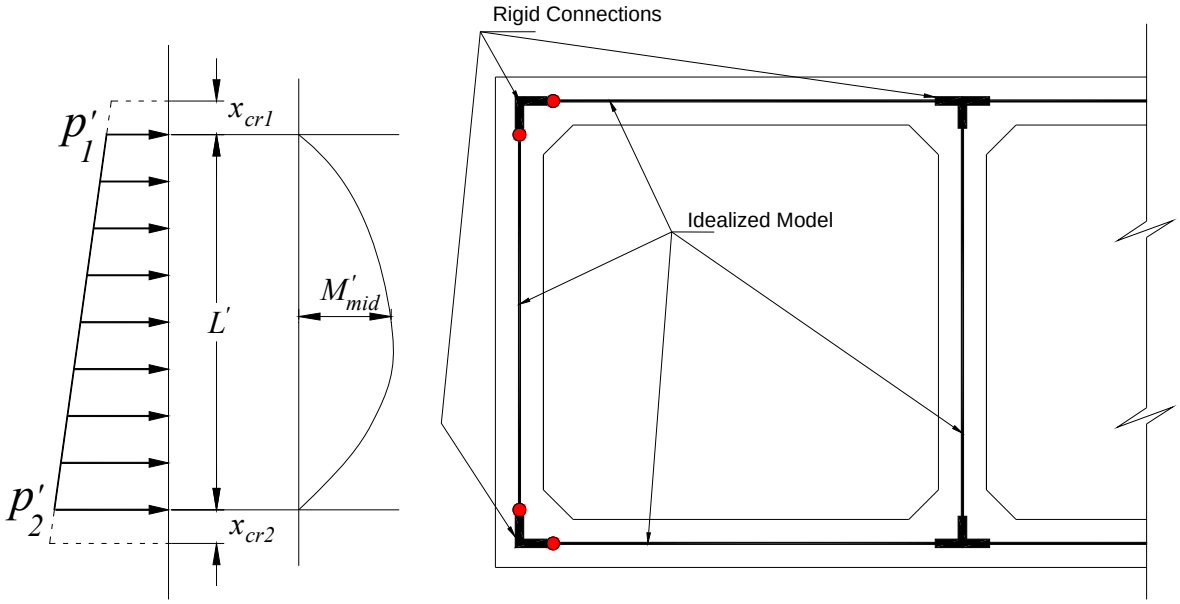

(b) Intermediate hinge at edge of rigid connection between slab and wall

Figure 29
Different 2D modeling assumptions for exterior wall

The ratio of M'_{mid} to M_{mid}, $\alpha = M'_{mid}\ / M_{mid}$, represents how much reduction in mid-height wall moment can be gained if the rigidity of the corner joints are taken advantage of. Obtaining the reduced moment value using a software that is not capable of modeling rigid links, can be obtained by reducing the applied pressures by the ratio α; i.e., use pressures αp_1

and αp_2. This is a modification that the user of the software can apply as an adjustment to the input in any software on a model similar to the one shown in Figure 30.

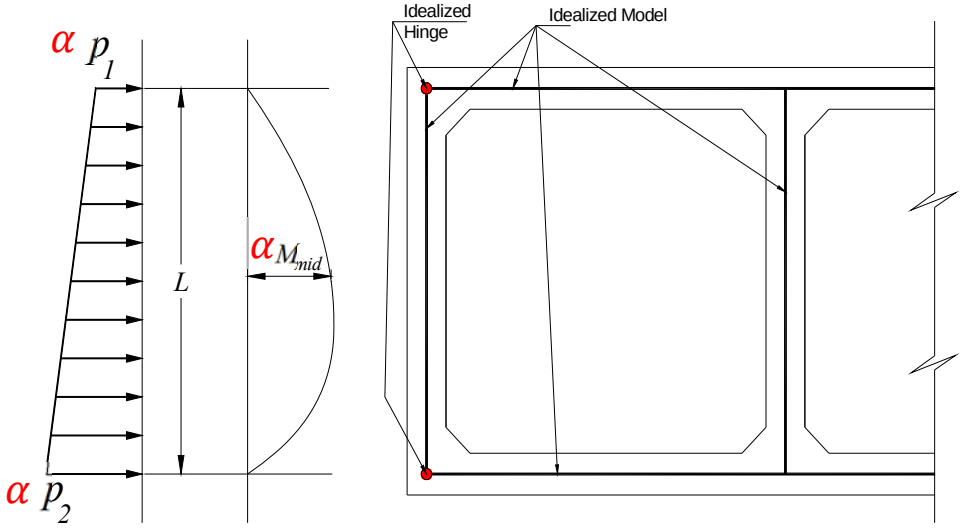

Figure 30
Modified earth pressures in 2D models with hinge at point of intersection between slab and wall

Figure 31 shows plots of the reduction factor, α, for different nominal box sizes and slab thicknesses assuming a haunch size equal to 6 in. if it exists. It can be seen that the reduction ranges between about 10% and 30% (see Figure 31-a) for the conservative assumption that no haunches exist at the top and bottom corners; i.e. the intermediate hinge is at the edge of the slab connection with the exterior wall. For the typical Louisiana old standard configuration (a haunch exists at the top corners while no haunch at the bottom corner with the hinge taken at 2/3 of the haunch size – $k_1 = 2/3$ and $k_2 = 0$), it can be seen that the reduction ranges between about 15% and 40% as can be seen in Figure 31-b. Finally, if haunches exist at the top and bottom connections; i.e., $k_1 = k_2 = 2/3$, a higher reduction is to be expected in the range from 20% and 50% as can be seen in Figure 31-c.

It should be noted that even if such features are included in 2D models, they will not address the conservativism in the distribution width formulas currently adopted in AASHTO-LRFD. Nevertheless, small reductions in straining actions as a result of more realistic models can still help improve load rating of some culverts.

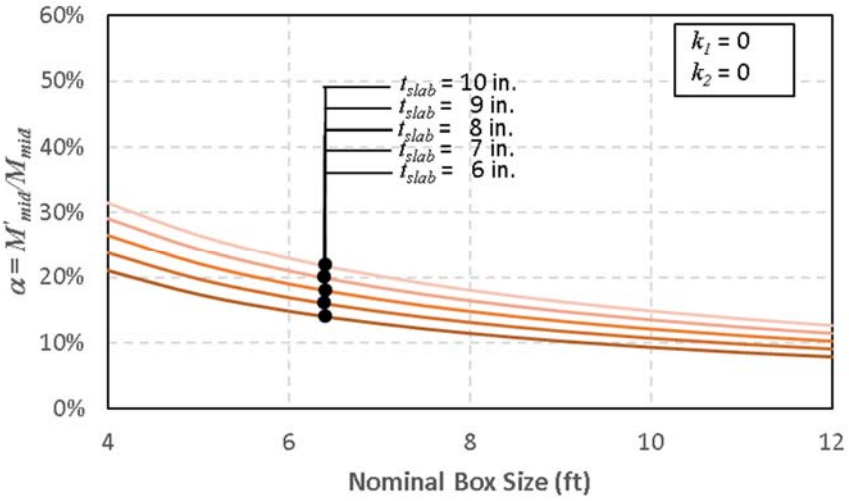

(a) Intermediate hinge at point of intersecetion between slab and wall

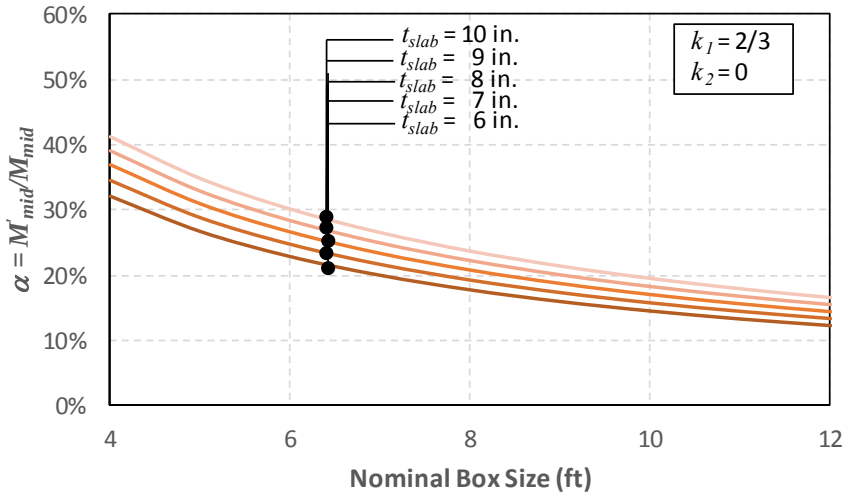

(b) Intermediate hinge at 2/3 of top haunch dimension and bottom point of intersecetion between slab and wall

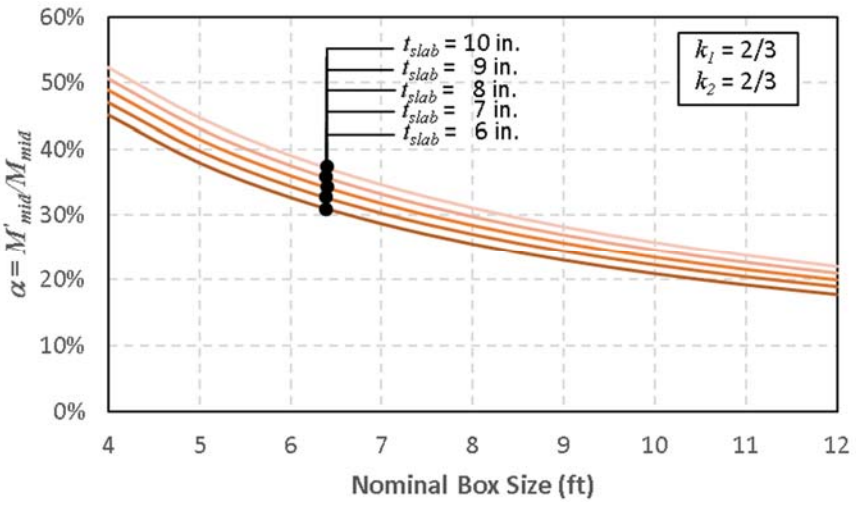

(c) Intermediate hinge at 2/3 of top and bottom haunch dimensions

Figure 31
Reduction factor for different box sizes and slab thicknesses

A similar approach can be used for the top slab by taking advantage of the horizontal portions of the rigid connections. This is illustrated in Figure 32 for a uniform pressure, p, case. In the figure, the exterior span length, which controls the load rating of many culverts will be reduced from L to L'' if the intermediate hinge is assumed at the edge of the rigid connection. Consequently, the bending moments and shear forces will be reduced, which can be calculated using a simple continuous beam analysis as shown in the figures, which also accounts for the stiffness of the intermediate wall using a rotational spring, $k_{\theta,intW}$. Comparing the moments and shear forces resulting from both models can be used to obtain a reduction factor, α_{slab}. The value of this factor will have to be determined on a case by case basis because of the larger number of parameters involved especially since the simple model is statically indeterminate; e.g., relative slab/wall stiffnesses, extent of applied pressure, shear or moment.

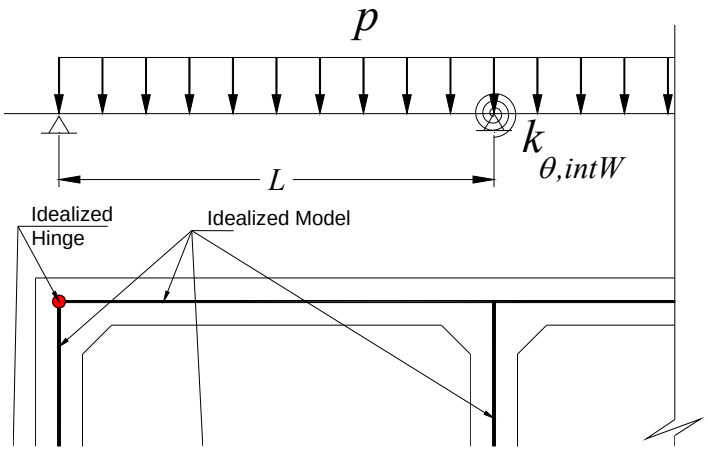

(a) Intermediate hinge at point of intersecetion between slab and wall

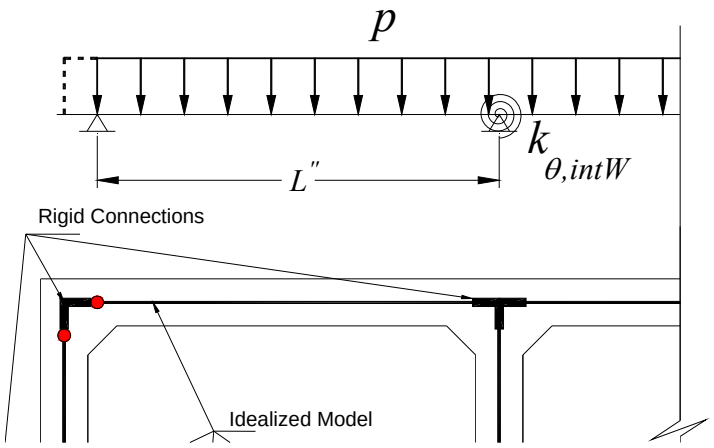

(b) Intermediate hinge at edge of rigid connection between slab and wall

Figure 32
Different 2D modeling assumptions for top slab

CONCLUSIONS AND RECOMMENDATIONS

Summary

Eight cast-in-place (CIP) reinforced concrete (RC) box culverts selected by LA DOTD were load tested to obtain their structural response using a 48-channel monitoring system under truck loading. Three-dimensional (3D) finite element (FE) models were built for each of the selected culverts based on their actual as-built configurations. The FE models were calibrated using field data for under the rolling truck load used during the load tests. AASHTO load distribution and load factors were then used to calculate the load rating factor for different trucks.

The results from this study were used to recommend a procedure for load rating CIP-RC box culverts that do not produce acceptable load rating factors using conventional methods. The steps of the recommended procedure are detailed in the Implementation section of this report. Furthermore, simple adjustments to conventional 2D modeling are proposed for cases where the software on hand does not allow incorporating advanced features such as rigid connections.

Conclusions

Based on the results of this study, the following conclusions may be drawn.

Specific Results for Tested Culverts

1. None of the eight culverts had a rating factor less than 1.0. Three culverts had an acceptable inventory level rating factor between 1.0 and 1.5, while the rest of the culverts had an inventory level rating factors above 1.5.

2. Three of the culverts' rating factors were calculated between 1.4 and 2.0 at the operating level, while the others had higher rating factors.

3. The rating factors for all legal trucks were all above 1.0 with the lowest rating factor being 1.60.

General Observations based on Performance of Tested Culverts

1. In general, there were not any major structural cracks in the selected culverts; i.e., caused by flexural moments due to gravity loads, observed in sections that the research team inspected.

2. Heavier trucks (i.e., higher GVW) do not necessarily provide controlling rating

factor. Instead, single axle load and neighboring axle spacing are the critical parameters to obtain the minimum rating factor.

3. Low fill height culverts and larger spans are more susceptible to lower load rating factors.

4. The controlling section that produces the minimum rating factor is typically the midspan (moments) in exterior cell slabs.

5. AASHTO LRFD live load distribution for flexible pavements be conservatively used to capture real load effects on 3D FE models. Concrete pavements provide additional distribution of wheel loads. With more advanced modeling features (e.g., stiff plate on soil fill), it may be possible to take advantage of this additional load distributing element.

6. Backfill soil springs reduce the exterior span forces and displacements due to live load effects. Thus, neglecting the backfill provides conservative load rating factor for the critical sections located in exterior span.

7. Soil-structure interaction in cast in place culverts does not appear to a provide major change in rating factor for the tested culverts. This may not be a general conclusion as the dimensions of the tested culverts are considered to be on the low end. Larger culverts may exhibit a different behavior.

8. Strain levels measured during live load testing indicate that the tested culverts are probably subjected to load levels below their cracking load levels, which implies that the culvert elements are behaving as uncracked RC sections.

Recommendations

Based on the results presented in this report for load rating eight CIP-RC culverts, it can be said that many culverts with rating challenges are very likely to have acceptable rating factors as demonstrated by the field tests and refined 3D FE models. Refined models should only be used after exhausting the use of the simpler 2D models if they do not result in acceptable rating factors. A procedure giving the details and procedure for load rating CIP-RC box culverts is provided in the "Implementation Statement" section.

Given that refined models (3D FE) are expensive and not practical for implementation in load rating all culverts in the inventory, and that producing 2-dimensional (2D) models that take advantage of all load distribution sources (i.e., soil and structural) was not part of the

scope of this study, it is recommended that a follow up study should be focused on calibrating 2D models to produce better results than what current AASHTO equations deliver. Such a study should also attempt to produce rating tables for categories of CIP-RC box culverts for a wide range of box dimensions, earth fill height, and concrete strength.

ACRONYMS, ABBREVIATIONS & SYMBOLS

AASHTO	The American Association of State Highway and Transportation Officials
ADT	Annual daily traffic
A_r	Nominal axial resistance capacity
CIP	Cast-in-place
DC	Dead load effect due to structural components
DOT	Department of transportation
DOTD	Louisiana Department of Transportation and Development
DW	Dead load effect due to wearing surface
E_c	Modulus of elasticity of concrete
EH	horizontal earth pressure
E_{perp}	Tire contact width
ES	uniform earth surcharge
E_s	Modulus of elasticity of steel
E_{span}	Tire contact length
EV	Verical earth pressure
f_c'	Compressive strength of concrete
FH	Fill Height
GVW	Gross vehicle weight
IM	dynamic load allowance
k	Subgrade Winkler's spring stiffness
k_o	Coefficient of at-rest lateral earth pressure
k_1	Portion of haunch considered rigid (top corner)
k_2	Portion of haunch considered rigid (bottom corner)
$K_{\theta,int}$, $K_{\theta,ext}$	Internal and external rotational spring stiffness
L	Exterior wall structural length
L'	Exterior wall reduced structural length
L_{ext}	Total extended length
L_i	Original strain gauge length (3 in.) without extension
LL	live load effect
LRFD	Load and Resistance Factor Design
LS	live load surcharge
LTRC	Louisiana transportation research center
LVDT	Linear variable differential transformer
MBE	The Manual for Bridge Evaluation
M_{cr}	Cracking moment

M_r	Nominal moment resistance capacity
M_{mid}	Exterior wall midspan moment assuming hinges at wall slab intersection
M'_{mid}	Exterior wall midspan moment assuming hinges at rigid connection edge
NCHRP	National Cooperative Highway Research Program
N_{lp}	Number of load tested truck path
$n_{lp,i}$	Number of sensors used in one load path
P	Single truck axle load
PCA	Portland Cement Association
pci	Pounds per cubic in.
RF	Rating factor
R_n	Nominal member resistance
V_r	Nominal shear resistance capacity
WS	Wearing surface
x_{cr1}	Length of rigid connection (top corner)
x_{cr2}	Length of rigid connection (bottom corner)
y_{exp}	Sensor data obtained from field test
y_{FE}	Sensor data obtained from FE model
Δ	Exterior opening mid span deflection
γ_c	Density of reinforced concrete
γ_{DC}	LRFD load factor for structural components
γ_{DW}	LRFD load factor for wearing surface
γ_{EH}	LRFD load factor for horizontal earth pressure
γ_{ES}	LRFD load factor for uniform earth surcharge
γ_{EV}	LRFD load factor for verical earth pressure
γ_{LL}	Evaluation live load factor
γ_{LS}	LRFD load factor for live load surcharge
ψ_s	Sensor data correction factor for extended strain gauges
$\mu\varepsilon$	microstrain
ϕ	LRFD resistance factor
ϕ_c	Condition factor
ϕ_s	System factor

REFERENCES

1. Petersen, D. L., Nelson, C. R., Li, G., McGrath, T. J., and Kitane, Y. R*ecommended Design Specifications for Live Load Distribution to Buried Structures*. The National Academies Press, Washington, DC, 2010.

2. ACPA. *Concrete Pipe Design Manual.* American Concrete Pipe Association, Texas, 2007 .

3. AASHTO. *Standard Specifications for Highway Bridges*. American Association of State Highway and Transportation Officials, Washington, D.C., 2002.

4. AASHTO. *LRFD Bridge Design Specifications*. American Association of State Highway and Transportation Officials, Washington, D.C., 2014.

5. Abdel-Karim, A. M., Tadros, M. K., and Benak, J. V. "Live Load Distribution on Concrete Box Culverts." *Transportation Research Record*, No. 1288, 1990, pp. 136-151.

6. McGrath, T. J., Liepins, A. A., and Beaver, J. L. "Live Load Distribution Widths for Reinforced Concrete Box Section." *Journal of the Transportation Research Board*, 2005, pp. 99-108.

7. Abolmaali, A. and Garg, A. K. "Effect of Wheel Live Load on Shear Behavior of Precast Reinforced Concrete Box Culverts." *Journal of Bridge Engineering,* Vol. 13, No. 1, 2008, pp. 93-99.

8. Orton, S. L., Loehr, J. E., Boeckmann, A., and Havens, G. "Live-Load Effect in Reinforced Concrete Box Culverts under Soil Fill." *Journal of Bridge Engineering,* Vol. 20, No. 11, 2015, p. 9.

9. Wood, T. A., Lawson, W. D., Jayawickrama, P. W., and Newhouse, C. D. "Evaluation of Production Models for Load Rating Reinforced Concrete Box Culverts." *Journal of Bridge Engineering,* Vol. 20, No. 1, 2015.

10. Wood, T. A., Lawson, W. D., Surles, J. G., Jayawickrama, P. W., and Seo, H. "Improved Load Rating of Reinforced-Concrete Box Culverts Using Depth-Calibrated Live-Load Attenuation." *Journal of Bridge Engineering,* Vol. 21, No. 12, 2016.

11. Acharya, R., Han, J., and Parsons, R. L. "Numerical Analysis of Low-Fill Box Culvert under Rigid Pavement Subjected to Static Traffic Loading." *International Journal of Geomechanics,* Vol. 16, No. 5, 2016.

12. Acharya, R., Han, J., Brennan, J. J., Parsons, R. L., and Khatri, D. K. "Structural Response of a Low-Fill Box Culvert under Static and Traffic Loading." *Journal of Performance of Constructed Facilities,* Vol. 30, No. 1, 2016.

13. Frederick, G. R. and Tarhini, K. M. "Model Analysis of Box Culverts Subjected to Highway Loading." *Experimental Mechanics,* Vol. 29, No. 2, 1989, pp. 183-187.

14. Kinchen, R. W., Temple, W. H., and Lacinak, H. W. "*Evaluation of Drainage Pipe by Field Experimentation and Supplemental Laboratory Experimentation.*" Report No. 101, 1977.

15. Kinchen, R. W., Temple, W. H., Lacinak, H. W., and Gueho, B. J. "*Evaluation of Drainage Pipe by Field Experimentation and Supplemental Laboratory Experimentation.*" Report No. FHWA-LA-78-115, 1978.

16. Temple, W. H., Rasoulian, M., and Gueho, B. J. "*Evaluation of Drainage Pipe by Field Experimentation and Supplemental Laboratory Experimentation.*" Report No. 154, 1981.

17. Garber, J. D., Lin, J. H., and Smith, L. G. "*Feasibility of Applying Cathodic Protection of Culverts to Underground Culverts.*" Report No. FHWA/LA-91/238, 1991.

18. Garber, J. D., Lin, J. H., and Smith, L. G. "*Feasibility of Applying Cathodic Protection of Culverts to Underground Culverts.*" Report No. FHWA/LA-94/284, 1995.

19. Garber, J. D. and Smith, L. G. "*Cathodic Protection of Culverts - Field Inspection and Expert System* " Report No. LA-99/324, 1999.

20. AASHTO. *The Manual for Bridge Evaluation*. American Association of State Highway and Transportation Officials, Washington, D.C., 2011.

21. Wood, T., Newhouse, C. D., Jayawickrama, P., and Lawson, W. D. "*Evaluating Existing Culverts for Load Capacity Allowing for Soil Structure Interaction.*" Report No. 0-5849-1, 2010.

This public document is published at a total cost of $250
42 copies of this public document were published in this first printing at a cost of $250. The total cost of all printings of this document including reprints is $250. This document was published by Louisiana Transportation Research Center to report and publish research findings as required in R.S. 48:105. This material was duplicated in accordance with standards for printing by state agencies established pursuant to R.S. 43:31. Printing of this material was purchased in accordance with the provisions of Title 43 of the Louisiana Revised Statutes.